Mesoscopic fluctuations of the supercurrent in diffusive Josephson junctions

Manuel Houzet[1] and Mikhail A. Skvortsov[2]

[1]*Commissariat à l'Énergie Atomique, DSM/DRFMC/SPSMS, 38054 Grenoble, France*
[2]*Landau Institute for Theoretical Physics, Chernogolovka, Moscow region 142432, Russia*

We study mesoscopic fluctuations and weak-localization correction to the supercurrent in Josephson junctions with coherent diffusive electron dynamics in the normal part. Two kinds of junctions are considered: a chaotic dot coupled to superconductors by tunnel barriers and a diffusive junction with transparent normal-superconducting interfaces. The amplitude of current fluctuations and the weak-localization correction to the average current are calculated as functions of the ratio between the superconducting gap and the electron dwell energy, temperature, and superconducting phase difference across the junction. Technically, fluctuations on top of the spatially inhomogeneous proximity effect in the normal region are described by the replicated version of the σ model. For the case of diffusive junctions with transparent interfaces, the magnitude of mesoscopic fluctuations of the critical current appears to be nearly three times larger than the prediction of the previous theory, which did not take the proximity effect into account.

I. INTRODUCTION

At low temperatures, conductance of metals is due to electron scattering on impurities. The wave nature of electron motion reveals a number of quantum interference effects: the weak-localization (WL) correction[1] to the classical Drude conductance and universal sample-to-sample conductance fluctuations.[2,3] In mesoscopic samples whose size does not exceed the phase coherence length, $L_\phi(T)$, the magnitude of conductance fluctuations characterized by the root mean square (rms) δG is independent of the system size and degree of disorder and is of the order of the conductance quantum $G_Q = e^2/\pi\hbar$. Weak-localization corrections and universal conductance fluctuations have attracted considerable interest since the 1980s, both from the experimental and theoretical sides.[4]

Two years after the discovery of conductance fluctuations in metals, Altshuler and Spivak[5] applied the same idea to fluctuations of the supercurrent in Josephson junctions formed of a diffusive normal metal (N) placed between two superconducting (S) leads. They considered the limit of *long* junctions when the Thouless energy $E_T = \hbar D/L^2$ (D is the diffusion constant and L is the length of the junction) is much smaller than the superconducting gap Δ in the leads. In particular, it was found in Ref. 5, that for quasi-one-dimensional long wires, mesoscopic fluctuations of the critical current are characterized by the rms $\delta I_c = \sqrt{3\zeta(3)}eE_T/\pi\hbar = 0.60 eE_T/\hbar$ at zero temperature.

The theory of Ref. 5 was based on the standard diagrammatic technique operating with soft diffusive modes—diffusons and Cooperons—but Andreev reflection at the NS interface[6] was described by the *linear* phenomenological boundary conditions on diffusive modes.[7] However, the proximity effect in SNS systems is known to be essentially nonperturbative at low energies, where Cooper pairs penetrating from a superconductor strongly modify electronic properties and open a minigap E_* in the normal region.[8] This strong perturbation of the metallic state can be described only with the help of the full set of *nonlinear* Usadel

equations[9] (in diffusive systems). Thus, the treatment of Ref. 5, which effectively considered mesoscopic fluctuations of the supercurrent on top of a uniform metallic state without a minigap, is not accurate and should be reconsidered, taking the proximity effect into account nonperturbatively.[10]

Extensive studies of the proximity effect in SNS systems[11–14] demonstrate that the critical Josephson current is related to the minigap induced in the normal region: $I_c \sim GE_*/e$, where G is the normal-state conductance of the junction. On the other hand, the minigap can be roughly estimated as $E_* \sim \min(\Delta, E_{\rm dwell})$, where Δ is the superconducting gap, and $E_{\rm dwell} = \hbar/t_{\rm dwell}$ is the energy associated with the typical dwell time $t_{\rm dwell}$ of an electron in the normal region. Since mesoscopic fluctuations for quantum dots and quasi-one-dimensional systems are usually small in the parameter G_Q/G, one can estimate the magnitude of mesoscopic fluctuations as $\delta I_c \sim eE_*/\hbar$. For a long diffusive wire, $E_{\rm dwell} \sim E_T$, indicating that results of Ref. 5 are qualitatively correct.

The scattering-matrix approach[15] has proven to be a powerful tool for studying coherent electron transport in mesoscopic conductors. In the framework of this approach, an arbitrary scatterer can be described by a set of transparencies in each conduction channel. The main transport characteristics of a mesoscopic conductor, such as the conductance, shot noise power, and conductance of the NS junction, can be written as a linear statistics on the transmission eigenvalues, $\Sigma_n f(T_n)$.[15] Then, the corresponding weak-localization corrections and mesoscopic fluctuations can be determined from the knowledge of the average density and the correlation function of transmission eigenvalues. For a diffusive wire, they were obtained in Refs. 16 and 17. However, the Josephson current is generally *not* a linear statistics on T_n's. It is a linear statistics only for a *short* ($\Delta \ll E_T$) wire,[18]

$$I(\chi) = \frac{e\Delta^2}{2\hbar} \sin\chi \sum_n \frac{T_n}{\epsilon_n} \tanh\frac{\epsilon_n}{2kT},\qquad(1)$$

where χ is the superconducting phase difference and $\epsilon_n = \Delta[1 - T_n \sin^2(\chi/2)]^{1/2}$ is the energy of the Andreev bound

state. In this limit, one finds the following for the fluctuations of the critical current at zero temperature:[16,17] $\delta I_c \simeq 0.30(e\Delta/\hbar)$. The crossover between short and long wires was also considered numerically within the tight-binding model.[19]

Recently, the problem of mesoscopic fluctuations of the supercurrent in short junctions with weakly transparent NS interfaces was considered by Micklitz,[20] who used the machinery of the supersymmetric nonlinear σ model.[21] Within that approach, the average Josephson current is obtained at the level of the saddle point, which corresponds to the quasiclassical Usadel equations,[22] while mesoscopic fluctuations can be obtained from fluctuations around the saddle point. We believe that the functional σ-model approach is a proper tool for studying mesoscopic fluctuations of the Josephson current, especially in the limit of long junctions where the multiple scattering theory fails.

A couple of experiments with the use of a gated semiconductor instead of a normal metallic part have been reported.[23,24] Mesoscopic fluctuations were observed by varying the gate voltage. In Ref. 23, mesoscopic fluctuations were shown to follow precisely those of G, the latter being estimated from $I(V)$ curves at a bias voltage larger than the superconducting gap. On the other hand, δI_c was systematically found to be smaller than the theoretical estimate from Ref. 5. A similar behavior was reported in Ref. 24.

In this work, we present the derivation of mesoscopic fluctuations, $\delta I(\chi) = [\langle I^2(\chi)\rangle - \langle I(\chi)\rangle^2]^{1/2}$, and weak-localization correction, $\Delta_{\mathrm{WL}} I(\chi)$, to the Josephson current in diffusive SNS junctions within the replicated version of the nonlinear σ model. We ignore interaction effects in the normal metal and assume zero magnetic field. By expanding the action of the σ model around its saddle point, corresponding to an inhomogeneous solution of the Usadel equations, we present mesoscopic fluctuations in terms of the soft modes, analogous to Cooperons and diffusons in the normal state.[20,22] This approach allows us to follow the crossover between the regimes of short and long wires.

In general, we verify that for the Josephson current through a chaotic dot and a quasi-one-dimensional wire, $\delta I_c/I_c \sim -\Delta_{\mathrm{WL}} I_c/I_c \sim G_Q/G$, where G is the normal-state conductance of the system, and determine the exact coefficients in these relations as functions of the junction length and temperature. These coefficients are generally of the order of 1 but, in some cases (two tunnel barrier structures with low barrier transparency), are additionally suppressed.

In particular, we find that the approach of Ref. 5, which does not take the proximity effect into account, systematically underestimates rms I_c by the factor of order 3. In the limit of long $(E_T \ll \Delta)$ quasi-one-dimensional junctions at zero temperature we obtain

$$\delta I_c = 1.49 \frac{eE_T}{\hbar}, \tag{2}$$

which is 2.5 times larger than the prediction of Ref. 5. Similarly, for wide $(W_x, W_y \gg L)$ and long $(E_T \ll \Delta)$ three-dimensional junctions made of a metallic parallelepiped of size $L \times W_y \times W_z$, we find the following at $T=0$:

$$\delta I_c = 2.0 \frac{eE_T}{\hbar} \sqrt{\frac{W_y W_z}{L^2}}, \tag{3}$$

which is 2.8 times larger than the corresponding result of Ref. 5.

The paper is organized as follows. In Sec. II, we consider the case of a chaotic diffusive dot coupled to the superconducting leads through tunnel barriers. This model allows us to introduce the method and is simple enough to be solved analytically. In Sec. III, we consider the case of a diffusive wire with transparent NS interfaces. Mesoscopic fluctuations of the critical current in two-dimensional (2D) and three-dimensional (3D) geometries are calculated in Sec. IV. We compare our theory with available experimental data in Sec. V. The results are discussed in Sec. VI. Technical details are delegated to several Appendixes.

II. SUPERCONDUCTOR–CHAOTIC DOT–SUPERCONDUCTOR JUNCTIONS

As a warmup, in this section we consider a Josephson junction formed of a "zero-dimensional" chaotic dot in contact with two superconducting reservoirs through tunnel junctions with conductances G_L and G_R. A possible realization of this system would be a short diffusive wire, with the Thouless energy E_T much exceeding the superconducting gap Δ in the superconductors and with the intradot conductance $G_N = 2\pi G_Q E_T/\delta$ (where δ is the mean level spacing in the dot) much exceeding G_L and G_R. As a consequence, the conductance of the structure in its normal state is determined solely by the tunnel barriers: $G = G_L G_R/(G_L + G_R)$.

The average Josephson current in such a system has been studied by Aslamazov *et al.*[25] within the tunnel Hamiltonian approach, by Kupriyanov and Lukichev[26] with the help of the quasiclassical Usadel equations, and by Brouwer and Beenakker[27] using the scattering approach[18] and random matrix theory.[15] It was found that the amplitude of the supercurrent is controlled by the ratio between the superconducting gap Δ and the "escape" energy $E_g \sim G\delta/G_Q$. The later energy scale is associated with the broadening of levels in the dot due to coupling with the leads, playing here the role of the dwell energy E_{dwell} defined in the Introduction.

We shall rederive these results in the fermionic replica σ-model language and then use this formalism to study mesoscopic fluctuations of the Josephson current for the arbitrary ratio Δ/E_g. A similar approach was very recently followed by Micklitz,[20] who considered the effect of barrier transparencies on the average supercurrent and its fluctuation in the regime $\Delta \ll E_g$ within the framework of the supersymmetric σ model.

In Sec. II A, we introduce the replica σ model for this system. In Sec. II B, we analyze its saddle-point solution and rederive the quasiclassical result for the Josephson current. The fluctuation determinant is calculated in Sec. II C. It contains both weak-localization corrections to the supercurrent and its mesoscopic fluctuations, which are analyzed in Secs. II D and II E, respectively. The role of the charging effects is briefly discussed in Sec. II F. The results are summarized in Sec. II G.

A. Replica σ model for a chaotic dot

The equilibrium supercurrent which flows in a Josephson junction can be obtained from the free energy $\mathcal{F}=-kT \ln Z$ of the system at temperature T,

$$I(\chi) = \frac{2e}{\hbar} \frac{d}{d\chi} \mathcal{F}(\chi), \qquad (4)$$

where χ is the superconducting phase difference between the leads. Disorder averaging is performed in a standard way using the replica trick,[28]

$$\langle \mathcal{F}(\chi) \rangle = -kT \lim_{n \to 0} \frac{\langle Z_\chi^n \rangle - 1}{n}, \qquad (5)$$

where $\langle Z_\chi^n \rangle$ can be evaluated as a functional integral within the fermionic replica σ model,[29–31]

$$\langle Z_\chi^n \rangle = \int \mathcal{D}Q e^{-S[Q]}. \qquad (6)$$

The nonlinear σ model is a field theory formulated in terms of the matrix field Q acting in the direct product of the replica space of dimension n, infinite Matsubara energy space, two-dimensional Gorkov-Nambu space (Pauli matrices τ_i), and two-dimensional spin space (Pauli matrices σ_i). The Q matrix is subject to the nonlinear constraint $Q^2=1$ and obeys the charge conjugation symmetry,

$$Q = \bar{Q} \equiv \tau_1 \sigma_2 Q^T \sigma_2 \tau_1, \qquad (7)$$

where Q^T stands for the full matrix transposition. Condition (7) is related to the simultaneous introduction of the Gorkov-Nambu and spin spaces, which renders the vectors $\Psi = (\psi_\uparrow, \psi_\downarrow^*, \psi_\downarrow, -\psi_\uparrow^*)^T$ and Ψ^* linearly dependent. The functional integration in Q is performed over an appropriate real submanifold of the complex manifold defined by the constraints $Q^2=1$ and $Q=\bar{Q}$.

The action of the σ model for a chaotic dot coupled to the superconducting terminals via tunnel junctions is given by[32]

$$S[Q] = -\frac{\pi}{2\delta} \text{tr} \left(\epsilon\tau_3 Q + \sum_{i=L,R} \frac{G_i \delta}{4\pi G_Q} Q_i Q \right). \qquad (8)$$

Here, $\delta=(\nu V)^{-1}$ is the mean level spacing in the dot (V is the dot's volume and ν is the single-particle density of states at the Fermi energy per one spin projection), ϵ is the fermionic Matsubara energy, and the trace is taken over all spaces of the Q matrix.

In the superconducting reservoirs with the order parameters $\Delta e^{-i\chi/2}$ (left) and $\Delta e^{i\chi/2}$ (right), the matrices Q_i ($i=L,R$) are unit matrices in the replica and spin spaces, which are diagonal in the energy space with the matrix elements,

$$Q_{L,R} = \left(\tau_1 \cos \frac{\chi}{2} \pm \tau_2 \sin \frac{\chi}{2} \right) \sin \theta_s + \tau_3 \cos \theta_s, \qquad (9)$$

where $\cos \theta_s = \cos \theta_s(\epsilon) = \epsilon / \sqrt{\epsilon^2 + \Delta^2}$.

Equation (9) is often referred to as "the rigid boundary condition." It corresponds to neglecting the inverse proximity effect as well as depairing effect in the leads due to a finite current density (see, e.g., Ref. 14).
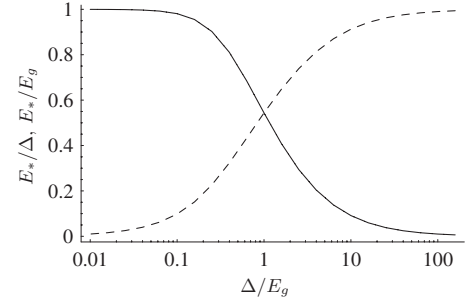

FIG. 1. The minigap E_* vs Δ/E_g in a superconductor–quantum dot–superconductor Josephson junction with symmetric tunnel barriers. The two curves correspond to E_* in units of Δ (solid line) and in units of E_g (dashed line).

B. Saddle point: Average Josephson current

We start the analysis of the σ model [Eq. (8)] with the saddle-point approximation, which amounts to neglecting mesoscopic fluctuations and weak-localization corrections. The matrix Q_0, which extremizes the action, solves the saddle-point equation,

$$\left[\epsilon\tau_3 + \sum_{i=L,R} \frac{G_i \delta}{4\pi G_Q} Q_i, Q_0 \right] = 0. \qquad (10)$$

Equation (10) is nothing but the Usadel equation for the quasiclassical Green's function for a chaotic dot supplied by the Kupriyanov-Lukichev boundary conditions[26] at the tunnel interface. This equation can also be obtained with the help of Nazarov's "circuit theory."[33]

The solution of Eq. (10) proportional to the unit matrix in the replica and spin spaces can be easily found,

$$Q_0 = (\tau_1 \cos \phi - \tau_2 \sin \phi)\sin \theta + \tau_3 \cos \theta, \qquad (11)$$

where

$$\tan \theta(\epsilon) = \frac{\Delta E_g(\chi)}{\epsilon(\sqrt{\epsilon^2 + \Delta^2} + E_g)}, \qquad (12a)$$

$$\tan \phi = \frac{G_R - G_L}{G_L + G_R} \tan \chi, \qquad (12b)$$

and

$$E_g(\chi) = \frac{\delta}{4\pi G_Q} \sqrt{G_L^2 + G_R^2 + 2G_L G_R \cos \chi}, \qquad (13)$$

with $E_g \equiv E_g(0)$. The pole of Q_0 located at imaginary ϵ is related to the minigap $E_*(\chi)$ in the density of states of the normal island.[8] In the limiting cases,

$$E_*(\chi) = \begin{cases} E_g(\chi), & \Delta \gg E_g \\ (\Delta/E_g)E_g(\chi), & \Delta \ll E_g, \end{cases} \qquad (14)$$

while in the intermediate region, $\Delta \sim E_g$, the dependence of E_* on χ is more complicated. In what follows, we will denote $E_* = E_*(0)$. Roughly speaking, $E_* \approx \min(\Delta, E_g)$ (see Fig. 1).

The action at the saddle point is given by nS_0, where n is the number of replicas and

$$S_0(\chi) = -\frac{2\pi}{\delta}\sum_\epsilon \omega_\epsilon(\chi), \qquad (15)$$

with the summation over the fermion Matsubara energies $\epsilon_p = \pi(2p+1)kT$, and

$$\omega_\epsilon(\chi) = \frac{\sqrt{\epsilon^2(\sqrt{\epsilon^2+\Delta^2}+E_g)^2+\Delta^2 E_g(\chi)^2}}{\sqrt{\epsilon^2+\Delta^2}}. \qquad (16)$$

In the leading order in $G/G_Q \gg 1$, one can neglect weak-localization and mesoscopic fluctuation effects (they will be studied in the next subsections). In this approximation, equivalent to the standard quasiclassical analysis, the Gaussian integral near the saddle point yields unity, and the average Josephson current can now be obtained from Eqs. (4)–(6) as $\langle I(\chi)\rangle_0 = (2ekT/\hbar)\partial S_0(\chi)/\partial\chi$, yielding

$$\langle I(\chi)\rangle_0 = \frac{\pi kT}{e}GE_g\sum_\epsilon \frac{\Delta^2\sin\chi}{(\epsilon^2+\Delta^2)\omega_\epsilon(\chi)}. \qquad (17)$$

The result [Eq. (17)] is certainly not new. It had been obtained previously by a number of authors.[20,25–27] Here, we simply rederive this result for completeness.

Symmetric junction. The general expression [Eq. (17)] is simplified for symmetric barriers: $G_L=G_R=2G$. In this case, $E_g(\chi)=E_g|\cos(\chi/2)|$ and $E_g=G\delta/\pi G_Q$. *At zero temperature* (more precisely, $kT\ll E_*$), the average Josephson current is controlled by the ratio Δ/E_g. When $\Delta\ll E_g$, the Josephson relation is not sinusoidal,

$$\langle I(\chi)\rangle_0 = \frac{G\Delta}{e}\sin\chi\,\mathbf{K}\!\left(\sin\frac{\chi}{2}\right), \qquad (18)$$

where $\mathbf{K}(x)=F(\pi/2,x)$ is the full elliptic integral of the first kind defined as in Ref. 34. The critical current $I_c \simeq 1.92G\Delta/e$ is achieved at a phase difference of $\chi_c \simeq 1.18(\pi/2)$.

In the opposite limit, $\Delta\gg E_g$, the Josephson relation is close to sinusoidal,

$$\langle I(\chi)\rangle_0 \simeq \frac{GE_g}{e}\sin\chi\ln\!\left(\frac{2\Delta}{E_g(\chi)}\right), \qquad (19)$$

with the critical current $I_c \simeq (GE_g/e)\ln(2\Delta/E_g)$ at a phase difference of $\chi_c \simeq \pi/2$.

The crossover for the critical current and critical phase at zero temperature and arbitrary relation between Δ and E_g is illustrated in Fig. 2.

At temperature close to the critical temperature of the leads, T_c, the superconducting gap vanishes as $\Delta(T) \propto k[T_c(T_c-T)]^{1/2}$. Then, for relevant energies $\epsilon\gtrsim kT\gg\Delta(T)$, Eq. (17) can be simplified, yielding a sinusoidal Josephson relation with the critical current

$$I_c = \begin{cases} (\pi G\Delta^2/4ekT_c), & \Delta\ll E_g \\ 7\zeta(3)GE_g\Delta^2/4e\pi^2k^2T_c^2, & \Delta\gg E_g, \end{cases} \qquad (20)$$

where $\zeta(3)\approx 1.202$ is the Riemann zeta function.

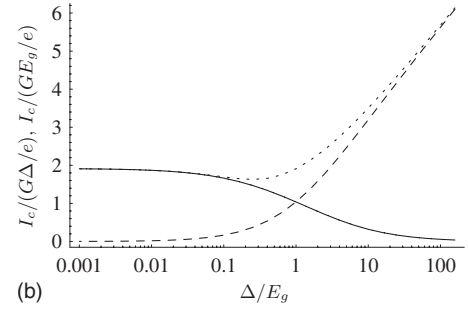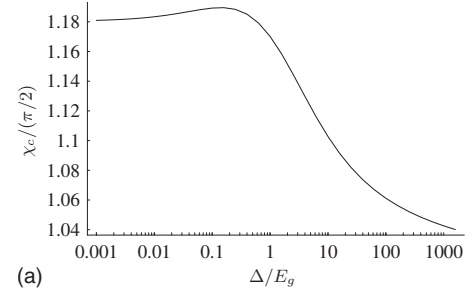*At intermediate temperatures*, $E_g\ll kT\ll kT_c$, we find I_c

FIG. 2. Quasiclassical results for a superconductor–quantum dot–superconductor Josephson junction with symmetric tunnel barriers: (a) the critical phase χ_c (in units of $\pi/2$) vs Δ/E_g at zero temperature; (b) the critical current I_c (solid line: in units of $G\Delta/e$, dashed line: in units of GE_g/e, dotted line: in units of GE_*/e) vs Δ/E_g at zero temperature.

$=(GE_g/e)\ln(2\gamma\Delta/\pi kT)$, where $\gamma=e^C=1.781,\dots$ is the Euler constant, in agreement with Refs. 25–27.

C. Gaussian fluctuations near the saddle point

In this subsection, we take Gaussian fluctuations near the saddle point into account. Since we will be interested in mesoscopic fluctuations of the Josephson current (see Sec. II E), we will have to consider the average $\langle Z_{\chi_1}^{n_1}Z_{\chi_2}^{n_2}\rangle$ of two partition functions calculated at different superconducting phases χ_1 and χ_2. This average can also be expressed in terms of the σ model,

$$\langle Z_{\chi_1}^{n_1}Z_{\chi_2}^{n_2}\rangle = \int \mathcal{D}Q e^{-S[Q]}, \qquad (21)$$

where the only difference with the σ model described in Sec. II A is that now Q becomes an $(n_1+n_2)\times(n_1+n_2)$ matrix in the replica space. Correspondingly, the superconducting Q matrices in the terminals should be modified. Now, they are diagonal in the replica space, having the superconducting phase difference χ_1 (χ_2) in the n_1 first (n_2 last) replicas. With these modifications, the action of the σ model has the same form [Eq. (8)].

At the saddle point, the matrix Q_0 extremizing the action is diagonal in the energy and replica spaces. Its diagonal elements are given by Eqs. (11), (12a), and (12b), where the phase χ is set to χ_1 (χ_2) if $1\le a\le n_1$ ($n_1<a\le n_1+n_2$), where a is a replica index.

In order to study fluctuations near this saddle point, we write matrices close to Q_0 as

$$Q = U^\dagger \Lambda (1 + W + W^2/2 + \cdots) U. \tag{22}$$

Here, matrices Λ and U should be chosen in such a way that in the absence of fluctuations, at $W=0$, Eq. (22) reduces to $U^\dagger \Lambda U = Q_0$. Usually, one has to require

$$\{\Lambda, W\} = 0 \tag{23a}$$

and impose the constraint following Eq. (7),

$$\bar{W} = -W \tag{23b}$$

and the requirement of convergency of the σ model on the perturbative level,

$$W^\dagger = -W. \tag{23c}$$

The form of the parametrization [Eq. (22)] is standard, while the choice of the matrix Λ is a matter of convenience. A possible choice could be the metallic saddle point,[31] $\Lambda_M = \tau_3 \, \mathrm{sgn}(\epsilon)$ [the limit of Eq. (9) at $\epsilon \gg \Delta$]. Here, we adopt an alternative choice proposed by Ostrovsky and Feigel'man,[35]

$$\Lambda = \tau_1, \tag{24}$$

corresponding to the superconducting saddle point [Eq. (9)] at zero energy and $\chi=0$. With this choice of Λ, the unitary matrix U in Eq. (22) is given by

$$U = e^{-i\tau_2(\pi/4 - \theta/2)} e^{-i\tau_3(\phi/2)}. \tag{25}$$

The choice of the parametrization with $\Lambda = \tau_1$ has two technical advantages: (i) The solution of constraint (23a) is independent of energy, and (ii) constraint (23b) can be easily resolved.

A general parametrization of matrix W satisfying constraint (23a) is given by

$$W_{mn} = \tau_3 \hat{d}_{mn} + \tau_2 \hat{c}_{mn}, \tag{26}$$

where $m=(\epsilon, a)$ and $n=(\epsilon', b)$ encode both the energy and replica indices, and $\hat{d}_{mn}$ and $\hat{c}_{mn}$ are 2×2 matrices in the spin space, which can be expanded in the Pauli matrices as

$$\hat{d} = d_0 + \mathbf{d}\boldsymbol{\sigma}, \quad \hat{c} = c_0 + \mathbf{c}\boldsymbol{\sigma}. \tag{27}$$

The variables d_0 and c_0 ($\mathbf{d}$ and $\mathbf{c}$) will be referred to as singlet (triplet) modes. They play the same role as diffusons and Cooperons in a normal metal, describing soft diffusive excitations on top of an inhomogeneous proximity-induced state. Note that contrary to diffusive modes in a normal metal, these d and c modes are generally coupled in the presence of a supercurrent in the normal region (see Sec. III).

Equations (23b) and (23c) yield

$$d_0 = d_0^T = -d_0^\dagger, \quad \mathbf{d} = -\mathbf{d}^T = -\mathbf{d}^\dagger, \tag{28a}$$

$$c_0 = -c_0^T = -c_0^\dagger, \quad \mathbf{c} = \mathbf{c}^T = -\mathbf{c}^\dagger. \tag{28b}$$

Here, transposition acts in the replica and energy spaces. In terms of the matrix elements, Eqs. (28a), e.g., read

$$(d_0)_{\epsilon,\epsilon'}^{ab} = (d_0)_{-\epsilon',-\epsilon}^{ba} = -(d_0^*)_{\epsilon',\epsilon}^{ba}, \tag{29a}$$

$$(d_i)_{\epsilon,\epsilon'}^{ab} = -(d_i)_{-\epsilon',-\epsilon}^{ba} = -(d_i^*)_{\epsilon',\epsilon}^{ba}. \tag{29b}$$

Independent integration variables for the singlet d_0 mode can be chosen, e.g., as

$$(d_0)_{\epsilon,\epsilon'}^{ab} \in \mathbb{C} \quad \text{if } a > b, \epsilon > 0,$$

$$(d_0)_{\epsilon,\epsilon'}^{aa} \in \mathbb{C} \quad \text{if } \epsilon > |\epsilon'| > 0,$$

$$(d_0)_{\epsilon,-\epsilon}^{aa} \in \mathbb{C} \quad \text{if } \epsilon > 0,$$

$$(d_0)_{\epsilon,\epsilon}^{aa} \in i\mathbb{R} \quad \text{if } \epsilon > 0,$$

and analogously for the triplet $c_{i=1,2,3}$. Independent integration variables for the triplet $d_{i=1,2,3}$ modes can be chosen, e.g., as

$$(d_i)_{\epsilon,\epsilon'}^{ab} \in \mathbb{C} \quad \text{if } a > b, \epsilon > 0,$$

$$(d_i)_{\epsilon,\epsilon'}^{aa} \in \mathbb{C} \quad \text{if } \epsilon > |\epsilon'| > 0,$$

$$(d_i)_{\epsilon,\epsilon}^{aa} \in i\mathbb{R} \quad \text{if } \epsilon > 0,$$

and analogously for the singlet c_0.

Expanding the action in the Gaussian approximation over fluctuations near the saddle point, one finds, in general,

$$S^{(2)} = \frac{\pi}{\delta} \sum_{mn} \sum_{i=0}^{3} (d_i^* \ c_i^*)_{mn} \hat{A}_{mn} \begin{pmatrix} d_i \\ c_i \end{pmatrix}_{mn}, \tag{30}$$

where $\hat{A}_{mn}$ is a symmetric [it can be symmetrized using relations (28)] matrix in the (d,c) space with the simple block structure in the replica space,

$$\hat{A}_{\epsilon\epsilon'}^{ab} = \begin{cases} A_{\epsilon\epsilon'}^{\chi_1\chi_1} & \text{if } a,b \leq n_1, \\ A_{\epsilon\epsilon'}^{\chi_1\chi_2} & \text{if } a \leq n_1 < b, \\ A_{\epsilon\epsilon'}^{\chi_2\chi_1} & \text{if } b \leq n_1 < a, \\ A_{\epsilon\epsilon'}^{\chi_2\chi_2} & \text{if } n_1 < a,b. \end{cases} \tag{31}$$

Matrix $\hat{A}$ does not depend on spin index i since the spin is conserved. Such a dependence will arise if one takes magnetic impurities or spin-orbit interaction in the normal region into account.

Due to the absence of the $(d_i)_{\epsilon,-\epsilon}^{aa}$ and $(c_0)_{\epsilon,-\epsilon}^{aa}$ modes, the matrix $\hat{A}_{\epsilon,-\epsilon}^{aa}$ should be diagonal in the (d,c) space,

$$A_{\epsilon,-\epsilon}^{\chi\chi} = \begin{pmatrix} (A_{\epsilon,-\epsilon}^{\chi\chi})^{dd} & 0 \\ 0 & (A_{\epsilon,-\epsilon}^{\chi\chi})^{cc} \end{pmatrix}. \tag{32}$$

We will see below that this is indeed the case [see Eqs. (36) and (65)].

Integration over independent variables of the d and c modes gives the fluctuation determinant,

$$\langle Z_{\chi_1}^{n_1} Z_{\chi_2}^{n_2} \rangle = \mathcal{M} e^{-n_1 \tilde{S}_0(\chi_1) - n_2 \tilde{S}_0(\chi_2)}, \tag{33}$$

where $\tilde{S}_0(\chi)$ contains the WL correction,

$$\widetilde{S}_0(\chi) = S_0(\chi) - \frac{1}{2}\sum_\epsilon \text{tr} \ln \frac{(A^{\chi\chi}_{\epsilon,-\epsilon})^{dd}}{(A^{\chi\chi}_{\epsilon,-\epsilon})^{cc}} \qquad (34)$$

[we write this expression in the most general way assuming that $(A^{\chi\chi}_{\epsilon,-\epsilon})^{dd}$ and $(A^{\chi\chi}_{\epsilon,-\epsilon})^{cc}$ might be operators, as in Sec. III; for a chaotic dot considered in this section, the trace in Eq. (34) can be omitted], whereas the prefactor $\mathcal{M}$ accounts for mesoscopic fluctuations,

$$\mathcal{M} = \prod_{\epsilon,\epsilon'} \frac{1}{(\det A^{\chi_1\chi_1}_{\epsilon\epsilon'})^{n_1^2}(\det A^{\chi_1\chi_2}_{\epsilon\epsilon'})^{2n_1n_2}(\det A^{\chi_2\chi_2}_{\epsilon\epsilon'})^{n_2^2}}. \qquad (35)$$

In Eq. (35), the product over ϵ and ϵ' should be taken over all Matsubara energies, and we have omitted the factors which are equal to 1 in the replica limit $n_{1,2} \to 0$ and thus do not depend on $\chi_{1,2}$.

For a superconductor–quantum dot–superconductor junction considered in this section, matrix $\hat{A}$ can be easily found by expanding Eq. (8) in W with the help of Eqs. (22), (23a)–(23c), and (24)–(26),

$$A^{\chi\chi'}_{\epsilon\epsilon'} = \frac{\omega_\epsilon(\chi) + \omega_{\epsilon'}(\chi')}{2}\hat{\Sigma}_0, \qquad (36)$$

where $\omega_\epsilon(\chi)$ is defined in Eq. (16) and $\hat{\Sigma}_0$ is the identity matrix in the (d,c) space.

The weak-localization correction to the Josephson current and its mesoscopic fluctuations are discussed in the next subsections.

D. Weak-localization correction

The weak-localization correction to the Josephson current, $\Delta_{\text{WL}}I(\chi) \equiv \langle I(\chi)\rangle - \langle I(\chi)\rangle_0$, can be found with the help of Eqs. (4), (5), (33), and (34),

$$\Delta_{\text{WL}}I(\chi) = -\frac{ekT}{\hbar}\frac{\partial}{\partial\chi}\sum_\epsilon \text{tr} \ln \frac{(A^{\chi\chi}_{\epsilon,-\epsilon})^{dd}}{(A^{\chi\chi}_{\epsilon,-\epsilon})^{cc}}. \qquad (37)$$

Since for a superconductor–quantum dot–superconductor junction, matrix $\hat{A}$ [see Eq. (36)] acts as a unit matrix in the (d,c) space, there is no weak-localization correction to the Josephson current.

The situation here is analogous to the absence of the weak-localization correction to the conductance of a double-barrier normal metal–quantum dot–normal metal junction.[36–38] There, the weak-localization correction is proportional to the single-channel transparency Γ and vanishes in the tunnel limit $\Gamma \to 0$, with $G = N\Gamma$ fixed (N is the number of channels). This fact had been recently discussed by Whitney,[39] who argued that the absence of the weak-localization correction is related to the smearing of the coherent-backscattering peak between transmission and reflection channels.

E. Mesoscopic fluctuations

With the help of the replica trick and relation (4), the current-current correlation function can be expressed as
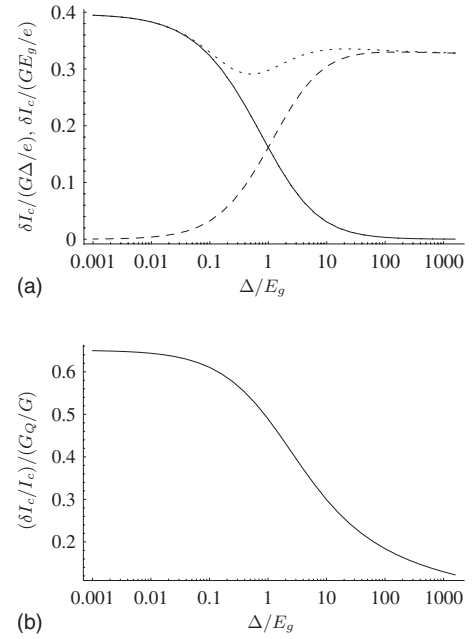

(a)

(b)

FIG. 3. (a) Mesoscopic fluctuations of the critical current, $\delta I_c = (\text{var } I_c)^{1/2}$ (solid line: in units of $e\Delta/\hbar$, dashed line: in units of $eE_g/\hbar$, dotted line: in units of $eE_*/\hbar$) vs Δ/E_g at zero temperature. (b) The ratio $G\delta I_c/G_Q I_c$ vs Δ/E_g at zero temperature.

$$\langle I(\chi_1)I(\chi_2)\rangle = \left(\frac{2ekT}{\hbar}\right)^2 \frac{\partial^2}{\partial\chi_1\partial\chi_2}\lim_{n_1,n_2\to 0}\frac{\langle Z^{n_1}_{\chi_1}Z^{n_2}_{\chi_2}\rangle}{n_1n_2}. \qquad (38)$$

Making use of Eqs. (33) and (35), we get the general expression for the cumulant $\langle\langle I(\chi_1)I(\chi_2)\rangle\rangle \equiv \langle I(\chi_1)I(\chi_2)\rangle - \langle I(\chi_1)\rangle\langle I(\chi_2)\rangle$,

$$\langle\langle I(\chi_1)I(\chi_2)\rangle\rangle = -8\left(\frac{ekT}{\hbar}\right)^2\frac{\partial^2}{\partial\chi_1\partial\chi_2}\sum_{\epsilon\epsilon'}\text{tr}\ln A^{\chi_1\chi_2}_{\epsilon\epsilon'}. \qquad (39)$$

Since $A^{\chi_1\chi_2}_{\epsilon\epsilon'}$ given by Eq. (36) appears to be diagonal in the (d,c) space, the evaluation of Eq. (39) for the quantum dot geometry is trivial, and we get

$$\langle\langle I(\chi_1)I(\chi_2)\rangle\rangle = \left(\frac{4ekT}{\hbar}\right)^2\sum_{\epsilon\epsilon'}\frac{1}{[\omega_\epsilon(\chi_1) + \omega_{\epsilon'}(\chi_2)]^2}\frac{\partial\omega_\epsilon}{\partial\chi_1}\frac{\partial\omega_{\epsilon'}}{\partial\chi_2}. \qquad (40)$$

In the limits $T=0$ and $\Delta \ll E_g$, Eq. (40) had been recently derived by Micklitz[20] using the supersymmetric σ-model approach.

As shown in Ref. 40, mesoscopic fluctuations of the *critical* current, δI_c, can be obtained as $\delta I_c = \delta I(\chi_c)$.

Symmetric junction. We now consider symmetric junctions. At zero temperature we find

$$\delta I_c = \begin{cases} 0.396(e\Delta/\hbar) & \text{if } \Delta \ll E_g \\ eE_g/\pi\hbar & \text{if } E_g \ll \Delta, \end{cases} \qquad (41)$$

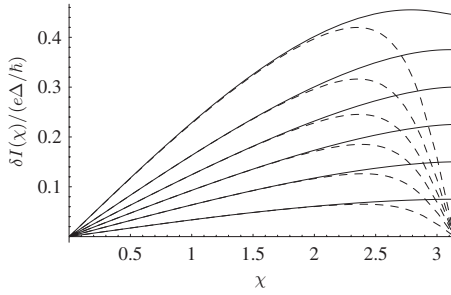while the result for an arbitrary ratio Δ/E_g is plotted in Fig. 3.

FIG. 4. Mesoscopic fluctuations of the Josephson current $\delta I(\chi)$ vs phase χ at zero temperature (solid line) and at temperature $kT = E_*/10$ (dashed line). The curves are plotted for different ratios Δ/E_g: 0 (top), 0.2, 0.5, 1, 2, 5 (bottom).

Equation (40) predicts a finite value of zero-temperature mesoscopic fluctuations at $\chi \to \pi$,

$$\delta I(\pi) = \frac{\sqrt{2}e}{\pi\hbar} \frac{\Delta E_g}{\Delta + E_g} \sim \frac{eE_*}{\hbar}, \quad (42)$$

which contradicts the general statement that the Josephson current must vanish exactly at $\chi = \pi$.[20,40] This is related to the breakdown of the Gaussian treatment of fluctuations at $\chi \to \pi$. Indeed, for a symmetric junction, the minigap $E_*(\chi)$ vanishes at $\chi = \pi$. Therefore, in the small vicinity of $\chi = \pi$, the mass [Eq. (36)] of the Gaussian fluctuations becomes comparable with the mean level spacing δ, and a more accurate analysis of the general nonlinear action [Eq. (8)] is required. Such an analysis should restore the exact relation $I(\pi) = 0$, resulting in vanishing fluctuations for $\chi \to \pi$. The width of the region where the Gaussian approximation fails can be estimated by expanding $\omega_\epsilon(\chi)$ [see Eq. (16)] at $\epsilon \ll \Delta$, $|\chi - \pi| \ll 1$,

$$\omega_\epsilon^2(\chi) \approx \left(1 + \frac{E_g}{\Delta}\right)^2 \epsilon^2 + \delta^2 \left(\frac{G}{4\pi G_Q}\right)^2 |\chi - \pi|^2. \quad (43)$$

Consequently, Eq. (40) cannot be applied in the region

$$T \ll \delta\Delta/(\Delta + E_g) \quad \text{and} \quad |\chi - \pi| \ll 4\pi G_Q/G. \quad (44)$$

Alternatively, the Josephson relation could be analyzed in terms of its harmonic content: $I(\chi) = \sum_{n>0} I_n \sin(n\chi)$. The above results imply that the mesoscopic fluctuation of I_n at large $n \gtrsim G/G_Q$ is overestimated at a very low temperature due to the failure of the Gaussian approximation at phase difference close to π.

Note that a small asymmetry of the junction, $|G_L - G_R| \gtrsim 4\pi G_Q$, generates a finite gap $E_g(\pi) \gtrsim \delta$, which restores the applicability of the Gaussian analysis and renders $\delta I(\pi) = 0$.

At a small temperature, $\delta I(\pi) = 0$, and the Josephson current decreases from its typical value [Eq. (42)] to 0 in the small phase range $|\chi - \pi| \lesssim kT/E_*$ (see Fig. 4).

Close to the critical temperature, T_c, when $\Delta(T) \to 0$, we find

$$\delta I_c^2 = \left(\frac{2ekT}{\hbar} \Delta^2(T) E_g^2\right)^2$$

$$\times \sum_{\epsilon,\epsilon'>0} \frac{1}{\epsilon^2 \epsilon'^2 (\epsilon + \epsilon' + 2E_g)^2 (\epsilon + E_g)(\epsilon' + E_g)}. \quad (45)$$

Thus,

$$\delta I_c = \begin{cases} (e\Delta^2(T)/8\hbar kT_c) & \text{if } kT_c \ll E_g \\ 0.010e\Delta^2(T)E_g^2/\hbar k^3 T_c^3 & \text{if } E_g \ll kT_c. \end{cases} \quad (46)$$

At intermediate temperatures such that $E_g \ll kT \ll kT_c$, we find

$$\delta I_c^2 = \left(\frac{2ekT}{\hbar} E_g^2\right)^2 \sum_{\epsilon,\epsilon'>0} \frac{1}{\epsilon\epsilon'(\epsilon + \epsilon')^2}. \quad (47)$$

Thus, $\delta I_c \simeq 0.12(eE_g^2/\hbar kT)$. This result was also obtained by means of the fourth order perturbation theory in the tunnel Hamiltonian connecting the wire to the leads, plus the random matrix theory on the statistics of eigenstates in the lead.[41]

F. Coulomb blockade effects and limits of validity

Results obtained above were derived assuming that electron-electron interaction effects in the dot can be neglected. In the presence of interaction, the phase on the dot becomes a fluctuating variable. The relative strength of the Coulomb interaction is characterized by the ratio between the charging energy $E_C = e^2/2C$ (C is the capacitance of the dot) and the Josephson energy $E_J \approx \hbar I_c/2e$. Results derived in this section apply in the limit of the *weak Coulomb blockade*, $E_C \ll E_J$, when interaction effects are small and can be treated perturbatively.[35] In the opposite limit of the *strong Coulomb blockade*, $E_C \gg E_J$, the superconductive proximity effect is strongly suppressed. Despite the fact that the minigap in the excitation spectrum becomes exponentially small in this regime,[35] the average supercurrent is only slightly reduced by interaction.[35,45] We expect that our results for the magnitude of mesoscopic fluctuations might be strongly modified in the strong Coulomb blockade regime. For instance, strong mesoscopic fluctuations of the supercurrent were predicted[42,43] and observed[44] in weakly coupled quantum dots, at $G \ll G_Q$, in the Coulomb blockade regime.

Our treatment of fluctuations is based on the Gaussian approximation controlled by the large dimensionless conductance $G/G_Q \gg 1$. Possible instanton effects, which are exponentially small in G/G_Q, have been neglected. For symmetric junctions, the Gaussian approximation breaks down in a narrow region [Eq. (44)] close to $\chi = \pi$ at low temperatures.

G. Summary of results

The results of our study are summarized in Table I. We note that, quite generally, the critical current at low temperatures is related to the minigap in the dot at $\chi = 0$, $E_* \sim \min(E_g, \Delta)$, through an Ambegaokar-Baratoff-like formula: $I_c \sim GE_*/e$, where G is the normal-state conductance

TABLE I. Summary of results for a quantum dot contacted symmetrically to superconducting leads ($G_L = G_R = 2G$). [Here, $g = G/G_Q$, $\Delta(T) = [(8\pi^2/7\zeta(3))k^2 T_c(T_c - T)]^{1/2}$, and $\gamma = 1.781, \ldots$.]

	$\chi_c/(\pi/2)$	eI_c/G	$\Delta_{WL}I(\chi)$	$\hbar\delta I_c/e$	$g\delta I_c/I_c$
$\Delta \ll E_g$, $T=0$	1.18	1.92Δ[a,b]	0	0.396Δ[c]	0.648
$E_g \ll \Delta$, $T=0$	1	$E_g \ln(2\Delta/E_g)$[b]	0	E_g/π	$1/\ln(2\Delta/E_g)$
Arbitrary E_g/Δ, $T=0$	Fig. 2(a)	Fig. 2(b)	0	Fig. 3(a)	Fig. 3(b)
$kT \lesssim kT_c \ll E_g$	1	$\pi\Delta^2(T)/4kT_c$[a]	0	$\Delta^2(T)/8kT_c$	1/2
$E_g \ll kT \lesssim kT_c$	1	$0.213E_g\Delta^2(T)/(kT_c)^2$[a]	0	$0.010\Delta^2(T)E_g^2/(kT_c)^3$	$0.15E_g/kT_c$
$E_g \ll kT \ll kT_c$	1	$E_g \ln(2\gamma\Delta/\pi kT)$[a,b,d]	0	$0.12E_g^2/kT$	$0.38E_g/[kT\ln(2\gamma\Delta/\pi kT)]$

[a]Reference 26.
[b]Reference 27.
[c]Reference 20.
[d]Reference 25.

of the system (up to a logarithmic factor for $E_g \ll \Delta$).

In a normal metallic double-barrier structure, conductance fluctuations are "universal," $\delta G = G_Q/2$, while weak-localization corrections vanish at infinitely small mean level spacing in the dot.[36–38]

In an S–quantum dot (QD)–S junction, we find that the WL correction to the Josephson current also vanishes, while the amplitude of mesoscopic fluctuations can be estimated as $\delta I_c/I_c \sim \delta G/G$, provided that $kT_c \ll E_g$. In the opposite limit, for poorly conducting barriers, mesoscopic fluctuations are additionally suppressed.

Note that in the limit $kT \lesssim kT_c \ll E_g$, we have $\delta I_c/I_c = \delta G/G$. This should be attributed to the fact that in this limit the Josephson relation becomes sinusoidal and proportional to the conductance of the system. Indeed, using Eq. (1) with $\Delta(T) \ll kT$, we find $I(\chi) = I_c \sin \chi$, where the critical current is proportional to the exact conductance before disorder averaging: $I_c = [e\Delta^2(T)/4\hbar kT]\Sigma_n T_n = \pi\Delta^2(T)G/4ekT$.

III. SUPERCONDUCTOR–NORMAL METAL–SUPERCONDUCTOR JUNCTIONS

We turn now to the case of a diffusive metallic wire connected to superconducting leads by transparent interfaces (the interface resistances are much lower than the resistance of the wire in the normal state). Proximity effect in such a geometry can be described by the diffusive replica σ model with the action[21,31]

$$S[Q] = \frac{\pi\nu}{8} \int d\mathbf{r}\, \text{tr}[D(\boldsymbol{\nabla}Q)^2 - 4\epsilon\tau_3 Q], \quad (48)$$

where D is the diffusion coefficient. At the boundaries with superconductors, we require that Q match with the Q_i matrices in the leads given by Eq. (9).

In this section, we concentrate on a quasi-one-dimensional geometry, when the length of the wire, L, much exceeds its transverse dimensions. Then, the spatial dependence of Q is reduced to the dependence on the coordinate x along the wire, which will be measured in units of L. The action of Eq. (48) can be written as

$$S[Q] = \frac{G_N}{16G_Q} \int_{-1/2}^{1/2} dx\, \text{tr}[(\nabla Q)^2 - 4\varepsilon\tau_3 Q], \quad (49)$$

where $G_N = 2\pi G_Q E_T/\delta$ is the normal-state conductance of the wire and $\varepsilon = \epsilon/E_T$ stands for Matsubara energies measured in units of the Thouless energy, $E_T = \hbar D/L^2$.

Following the same line as in Sec. II, we derive the quasiclassical Josephson relation as the saddle point of the action of Eq. (49) in Sec. III A. We find that the amplitude of the critical current is controlled by the ratio between Δ and E_T. Then, we express mesoscopic fluctuations and WL correction to the Josephson current in terms of Gaussian fluctuations in the vicinity of the nonuniform saddle point in Sec. III B. Interaction effects and limits of validity of our analysis are discussed in Sec. III C. Results are summarized in Sec. III D.

A. Josephson relation

At the saddle point, matrix $Q_0(x)$, which extremizes the action of Eq. (49), solves the Usadel equation,

$$-\nabla(Q_0 \nabla Q_0) + \varepsilon[\hat{\tau}_3, Q_0] = 0. \quad (50)$$

With the parametrization [Eq. (11)], this equation can be reduced to two differential equations:

$$\nabla(\sin^2 \theta \nabla \phi) = 0, \quad (51a)$$

$$\nabla^2\theta - 2\varepsilon \sin \theta - (\nabla\phi)^2 \sin \theta \cos \theta = 0, \quad (51b)$$

with the boundary conditions $\theta(\pm 1/2) = \theta_s$ and $\phi(\pm 1/2) = \pm \chi/2$. The Usadel angles at energies $\pm\varepsilon$ are related by the symmetries

$$\theta_{-\varepsilon} = \pi - \theta_\varepsilon, \quad \phi_{-\varepsilon} = \phi_\varepsilon. \quad (52)$$

According to Eq. (51a), $J = \sin^2 \theta \nabla \phi$ (usually referred to as the spectral current) is constant along the wire. Integrating Eq. (51b) then, we obtain

$$(\nabla\theta)^2 = 4\varepsilon[\cos \theta(0) - \cos \theta] + \frac{J^2}{\sin^2 \theta(0)} - \frac{J^2}{\sin^2 \theta}. \quad (53)$$

This last equation can be solved in quadratures, the implicit solution being given in terms of elliptic integrals. Its form is
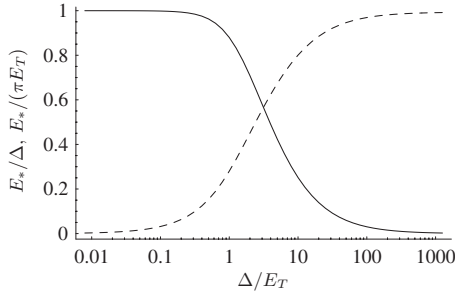
FIG. 5. The minigap E_* induced in the normal wire at $\chi=0$ (solid line: in units of Δ; dashed line: in units of πE_T) vs Δ/E_T.

FIG. 6. Josephson relation $I(\chi)$ (in units of $G_N\Delta/e$) for a short wire at zero temperature.

rather cumbersome and can be found in Appendix A. In a general case, J and $\theta(0)$ at given boundary conditions can be found only numerically. Note, however, that their determination requires a solution of only an algebraic rather than a differential equation.

Equation (53) can be used to determine the minigap E_* induced in the normal region due to the proximity effect. To this end, one has to perform analytic continuation $\epsilon \to -iE$ and search for the energy E_* when $\cos\theta$ first acquires a finite real part, indicating a nonzero density of states above E_*. The determination of the minigap simplifies for $\chi=0$. To solve the Usadel equation, we then introduce $\theta = \pi/2 + i\psi$ and get the relation between E and the value $\psi(0)$ at the center of the wire,

$$\sqrt{\frac{E}{E_T}} = \int_{\mathrm{arctanh}(E/\Delta)}^{\psi(0)} \frac{d\psi}{\sqrt{\sinh\psi(0) - \sinh\psi}}. \tag{54}$$

Equation (54) establishes a relation between E and $\psi(0)$. The value of E_* should be determined from the condition that Eq. (54) ceases to have real solutions for $\psi(0)$. For short wires ($\Delta \ll E_T$), $E_* \approx \Delta$, whereas for long wires ($\Delta \gg E_T$), $E_* \approx 3.122 E_T$,[46,47] in accordance with the general relation $E_* \sim \min(E_T, \Delta)$. The dependence of E_* on Δ/E_T is shown in Fig. 5.

The action at the saddle point $Q_0(x)$ is given by nS_0, where

$$S_0 = \frac{G_N}{4G_Q} \sum_\epsilon \int dx[(\nabla\theta)^2 + (\nabla\phi)^2 \sin^2\theta - 4\varepsilon\cos\theta]. \tag{55}$$

Taking the derivative with respect to χ, integrating by parts, and using the boundary conditions at $x = \pm 1/2$, we get $\partial_\chi S_0 = (G_N/2G_Q)\Sigma_\epsilon J$, yielding the quasiclassical expression for the supercurrent,

$$\langle I(\chi)\rangle_0 = \pi kT \frac{G_N}{e} \sum_\epsilon J. \tag{56}$$

Below, we evaluate the current [Eq. (56)] in different cases.

1. Short wire at zero temperature

The critical current for a short diffusive wire ($E_T \gg \Delta$) has been known for a long time.[11] In this case, the term propor-
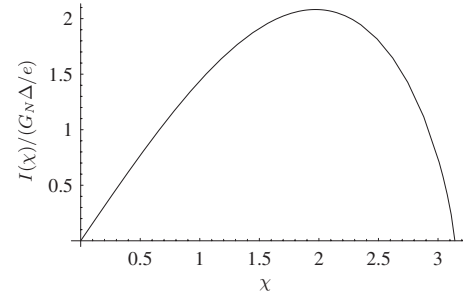
tional to ε in Eq. (51b) can be neglected, and the Usadel equation can be solved exactly,

$$\theta(x) = \arccos\left[\cos\theta(0)\cos\frac{Jx}{\sin\theta(0)}\right], \tag{57}$$

where

$$\sin\theta(0) = \frac{\sin\theta_s\cos\frac{\chi}{2}}{\sqrt{1 - \sin^2\theta_s\sin^2\frac{\chi}{2}}}, \tag{58a}$$

$$J = 2\sin\theta(0)\arcsin\left(\sin\theta_s\sin\frac{\chi}{2}\right). \tag{58b}$$

Calculating the supercurrent with the help of Eq. (56) at $T=0$, we get[11]

$$I(\chi) = \frac{\pi G_N\Delta}{e}\cos\frac{\chi}{2}\,\mathrm{arctanh}\left(\sin\frac{\chi}{2}\right). \tag{59}$$

Alternatively, this result can be obtained[48] by averaging the short-junction expression [Eq. (1)] over the Dorokhov distribution[49] of transmission eigenvalues T_n: $\mathcal{P}(T) = (G_N/2G_Q)/T\sqrt{1-T}$.

The Josephson relation [Eq. (59)] is nonsinusoidal (see Fig. 6). The critical current $I_c = 2.082 G_N\Delta/e$ is achieved at the critical phase $\chi_c = 1.255(\pi/2)$. At $\chi \to \pi$, the supercurrent vanishes but with a divergent derivative: $I(\chi) \sim I_c(\pi - \chi)\ln 1/(\pi-\chi)$.

2. Arbitrary wire at temperature close to T_c

At temperatures close to the critical temperature in the leads, T_c, the superconducting gap Δ in the leads is small: $\Delta(T) = [(8\pi^2/7\zeta(3))k^2T_c(T_c-T)]^{1/2} \ll kT$. Thus, at relevant energies $\epsilon \gtrsim kT \gg \Delta$, the anomalous (Gor'kov) component of the Green function is small, and the Usadel equation [Eq. (51b)] can be linearized with respect to $\sin\theta$. Its solution has the form

$$\sin \theta(x) e^{i\phi(x)} = \frac{\Delta}{|\epsilon|} e^{-i\chi/2} \frac{\sinh \kappa \left(\frac{1}{2} - x \right)}{\sinh \kappa}$$

$$+ \frac{\Delta}{|\epsilon|} e^{i\chi/2} \frac{\sinh \kappa \left(\frac{1}{2} + x \right)}{\sinh \kappa}, \quad (60)$$

where $\kappa = \sqrt{2|\varepsilon|} = \sqrt{2|\epsilon|/E_T}$. Calculating the spectral current with the help of Eqs. (D1) and (D2), we get

$$J = \frac{\Delta^2}{\epsilon^2} \frac{\kappa}{\sinh \kappa} \sin \chi. \quad (61)$$

Close to T_c, junctions are classified as short or long depending on the ratio between kT_c and E_T. For short junctions, $[\Delta(T) \ll kT \lesssim kT_c \ll E_T]$, the supercurrent is given by

$$I(\chi) = \frac{\pi G_N}{4e} \frac{\Delta^2}{kT} \sin \chi. \quad (62)$$

For long junctions $[\Delta(T), E_T \ll kT \lesssim kT_c]$, the supercurrent is exponentially suppressed,

$$I(\chi) \simeq \frac{8 G_N}{e} \frac{\Delta^2}{\sqrt{2\pi kT E_T}} \exp \left(- \sqrt{\frac{2\pi kT}{E_T}} \right) \sin \chi. \quad (63)$$

In both cases, the Josephson relation is sinusoidal.

3. Arbitrary wire at zero temperature

At $T=0$, the Josephson relation $I(\chi)$ depends only on the ratio between Δ and E_T. Short junctions were considered in Sec. III A 1. For arbitrary Δ/E_T, the critical current and critical phase obtained numerically are shown in Fig. 7.[13] Specifically, for long junctions ($E_T \ll \Delta$), the Josephson relation is still highly nonsinusoidal (see Fig. 8), with the critical current $I_c = 10.83 G_N E_T/e$ achieved at the critical phase $\chi_c = 1.271(\pi/2)$.[13]

B. Mesoscopic fluctuations and weak-localization correction

Fluctuations near the saddle point $Q_0(x)$ can be parametrized using Eqs. (22), (25), and (26). Substituting these expressions into the action of Eq. (49) and expanding to the second order in the modes $d(x)$ and $c(x)$, we get the following similar to Eq. (30):

$$S^{(2)} = \frac{G_N}{4G_Q} \int dx \sum_{mn} \sum_{i=0}^{3} (d_i^* \, c_i^*)_{mn} \hat{A}_{mn} \binom{d_i}{c_i}_{mn}. \quad (64)$$

The form of the operator $\hat{A}(x)$ is quite cumbersome [see Eq. (B2) in Appendix B]. Apart from the second derivative with respect to x, it contains also the first derivative. The latter can be eliminated by a proper unitary transformation [Eq. (B5)] mixing the d and c components of fluctuations. After such a rotation, the matrix $\hat{A}$ acquires the form[50]

$$\hat{A}_{mn}(x) = - \nabla^2 + \alpha_{mn} + \rho_{mn} \cos(\eta_m + \eta_n) \hat{\Sigma}_3$$

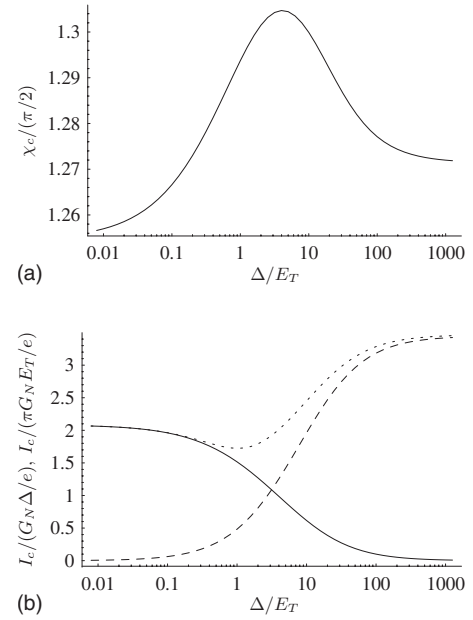$$+ \rho_{mn} \sin(\eta_m + \eta_n) \hat{\Sigma}_1, \quad (65)$$

where

FIG. 7. (a) The critical phase χ_c (in units of $\pi/2$) vs Δ/E_T at zero temperature. (b) The critical current I_c (solid line: in units of $G_N\Delta/e$, dashed line: in units of $\pi G_N E_T/e$, and dotted line: in units of $G_N E_*/e$) vs Δ/E_T at zero temperature.

$$\alpha_{mn} = \varepsilon_m \cos \theta_m - \frac{1}{4}[(\nabla \theta_m)^2 + (\sin \theta_m \nabla \phi_m)^2] + \varepsilon_n \cos \theta_n$$

$$- \frac{1}{4}[(\nabla \theta_n)^2 + (\sin \theta_n \nabla \phi_n)^2], \quad (66)$$

$$\rho_{mn} = \frac{1}{2} \sqrt{(\nabla \theta_m)^2 + (\sin \theta_m \nabla \phi_m)^2} \sqrt{(\nabla \theta_n)^2 + (\sin \theta_n \nabla \phi_n)^2}, \quad (67)$$

and the odd function $\eta_m(x)$ can be obtained by integrating the relation

$$\nabla \eta_m = - \frac{2\varepsilon_m J_m}{(\nabla \theta_m)^2 + (\sin \theta_m \nabla \phi_m)^2}. \quad (68)$$

Once the operator $\hat{A}$ is known, one can use the general equations [Eqs. (37) and (39)] to calculate the weak-
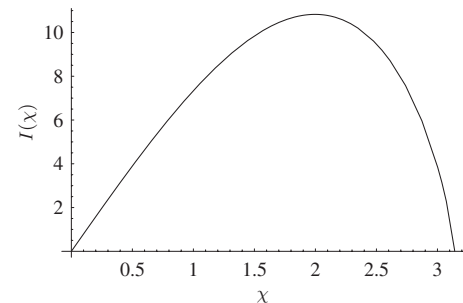

FIG. 8. Josephson relation $I(\chi)$ (in units of $G_N E_T/e$) for a long wire at zero temperature.

localization correction and mesoscopic fluctuations of the Josephson current. The only difference compared to the S-QD-S case is that now $\hat{A}(x)$ is an operator in the real space, and the determinant should be calculated with respect to spatial coordinates as well. In a general situation, for arbitrary Δ/E_T and temperatures, this can be done only numerically, following the procedure outlined in Appendix A. Several cases where a simple form of the operator $\hat{A}(x)$ allows for an analytic solution are discussed below. In Sec. III B 3, we present the results of a numeric solution for an arbitrary Δ/E_T at zero temperature.

1. Short wire

We start with the simplest case of a short wire, $\Delta \ll E_T$. This limit was analyzed previously in Refs. 16 and 17 using the scattering-matrix approach to the Josephson current.[18]

For short wires, the term proportional to ε in the Usadel equation can be neglected. Then, according to Eq. (53), $(\nabla\theta_m)^2 + (\sin\theta_m\nabla\phi_m)^2 = 4C_m^2$, where $C_m = J_m/2\sin\theta_m(0)$ is constant in the wire. With the same accuracy, Eq. (68) guarantees that $\eta_m(x) = 0$. As a result, the operator $\hat{A}$ in Eq. (65) becomes diagonal in the (d,c) space, with its diagonal elements being diffusion operators,

$$\hat{A}_{mn} = \begin{pmatrix} -\nabla^2 - (C_m - C_n)^2 & 0 \\ 0 & -\nabla^2 - (C_m + C_n)^2 \end{pmatrix}.$$

Since fluctuations must vanish in the reservoirs, the eigenvalues of $-\nabla^2$ are $\pi^2 p^2$ ($p = 1, 2, \ldots$), and the determinant of $A_{\varepsilon\varepsilon'}^{\chi_1\chi_2}$ involved in Eq. (39) can be readily obtained. As a result, the current-current correlation function acquires the form

$$\langle\langle I(\chi)I(\chi')\rangle\rangle = -8\left(\frac{ekT}{\hbar}\right)^2 \frac{\partial^2}{\partial\chi\partial\chi'}$$
$$\times \sum_{\epsilon\epsilon'} \ln \frac{\sin(C - C')}{C - C'} \frac{\sin(C + C')}{C + C'}, \quad (69)$$

where $C = \arcsin[(\Delta/\sqrt{\Delta^2 + \epsilon^2})\sin(\chi/2)]$ and C' is given by the same expression with $\varepsilon \to \varepsilon'$ and $\chi \to \chi'$.

At zero temperature, the sums over Matsubara energies reduce to integrals, and our expression for $\delta I^2(\chi) = \langle\langle I^2(\chi)\rangle\rangle = \text{var } I(\chi)$ becomes equivalent to the result of Refs. 16 and 17. The equivalence is explicitly demonstrated in Appendix C. For small χ, we have an expansion in powers of $\sin^2(\chi/2)$,

$$\delta I^2(\chi) = \left(\frac{e\Delta}{\hbar}\right)^2 \frac{\sin^2\chi}{30}\left(1 + \frac{62}{63}\sin^2\frac{\chi}{2} + \cdots\right). \quad (70)$$

The whole curve $\delta I(\chi)$ at $T=0$ is plotted in Fig. 9. Mesoscopic fluctuations of the critical current, $\delta I_c = \delta I(\chi_c)$, are characterized by $\delta I_c = 0.30 e\Delta/\hbar$.[16,17]

At zero temperature, the magnitude of mesoscopic fluctuations remains finite at $\chi = \pi$, $\delta I(\pi) = e\Delta/\pi\hbar$, contradicting the general symmetry requirement of vanishing $I(\pi)$. As in Sec. II E, this is related to the breakdown of the Gaussian treatment of fluctuations at $\chi \to \pi$. The most "dangerous" is
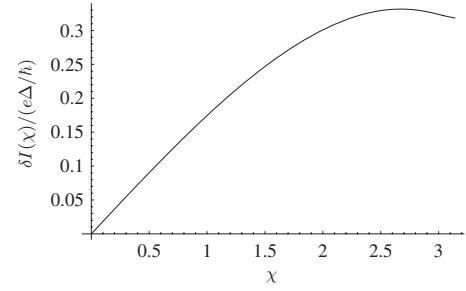

FIG. 9. Mesoscopic fluctuations $\delta I(\chi)$ (in units of $e\Delta/\hbar$) for a short wire at $T=0$.

the lowest ($p=1$) spatial mode A^{cc} with $\epsilon \ll \Delta$ at $\chi \to \pi$, whose mass is

$$\frac{A^{cc}}{2\pi} = \sqrt{\frac{\epsilon^2}{\Delta^2} + \frac{|\chi - \pi|^2}{4}} + \sqrt{\frac{\epsilon'^2}{\Delta^2} + \frac{|\chi' - \pi|^2}{4}}. \quad (71)$$

In the region [see Eq. (44)],

$$T \ll \Delta(G_Q/G_N) \quad \text{and} \quad |\chi - \pi| \ll G_Q/G_N, \quad (72)$$

Gaussian approximation fails and nonlinear effects become important, but the relative width of this region is small scaling as the inverse conductance. Finite temperatures render $\delta I(\pi) = 0$ and shrink the region of strong non-Gaussian fluctuations near $\chi = \pi$, which disappears at $kT \gg (G_Q/G_N)|\chi - \pi|\Delta$.

The weak-localization correction can be evaluated with the help of Eq. (37). Here, only c modes contribute to the result, and

$$\Delta_{\text{WL}}I(\chi) = \frac{ekT}{\hbar}\frac{\partial}{\partial\chi}\sum_\epsilon \ln\frac{\sin 2C}{2C}. \quad (73)$$

At zero temperature, we obtain

$$\Delta_{\text{WL}}I(\chi) = -\frac{e\Delta}{6\hbar}\sin\chi\left(1 + \frac{7}{15}\sin^2\frac{\chi}{2} + \cdots\right), \quad (74)$$

in agreement with Eq. (3.33) of Ref. 16. The whole dependence $\Delta_{\text{WL}}I(\chi)$ at $T=0$ is shown in Fig. 10. The WL correction to the critical current is $\Delta_{\text{WL}}I_c = -0.266 e\Delta/\hbar$.

At zero temperature, the WL correction [Eq. (73)] is discontinuous at $\chi = \pi$: $\Delta_{\text{WL}}I(\pi \mp 0) = \mp e\Delta/4\hbar$, which is again an artifact of the Gaussian approximation employed. The
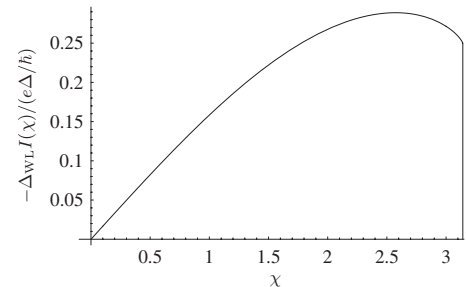

FIG. 10. Weak-localization correction $-\Delta_{\text{WL}}I(\chi)$ (in units of $e\Delta/\hbar$) for a short wire at $T=0$.

situation here is completely analogous to the situation with mesoscopic fluctuations discussed above.

2. Arbitrary wire at temperatures close to T_c

In Sec. III A 2, we have seen that the calculation of the quasiclassical Josephson current simplifies at temperatures close to T_c. The same occurs for mesoscopic fluctuations and WL correction. In order to calculate them, we decompose the operator $\hat{A}=\hat{A}_0+\hat{V}$ in Eq. (65) into a sum of the diffusion operator in the normal state, $\hat{A}_0=-\nabla^2+|\varepsilon_1|+|\varepsilon_2|$, and the perturbation $\hat{V}=\mathcal{O}(\Delta^2)$. Expanding $\mathrm{tr}\ln\hat{A}$ in powers of $\hat{V}$, we rewrite Eqs. (37) and (39) as

$$\Delta_{\mathrm{WL}}I(\chi)=-\frac{ekT}{\hbar}\frac{\partial}{\partial\chi}\sum_\epsilon \mathrm{Tr}\, G\hat{\Sigma}_3 V^{\chi\chi}_{\epsilon,-\epsilon},\tag{75}$$

$$\langle\langle I(\chi_1)I(\chi_2)\rangle\rangle=4\left(\frac{ekT}{\hbar}\right)^2\frac{\partial^2}{\partial\chi_1\partial\chi_2}\sum_{\epsilon_1\epsilon_2}\mathrm{Tr}(G\hat{V})^2,\tag{76}$$

where $\hat{G}=\hat{A}_0^{-1}$ is the Green function of the diffusion operator: $[-\nabla^2+|\varepsilon_1|+|\varepsilon_2|]G_{\varepsilon_1\varepsilon_2}(x,y)=\delta(x-y)$, and Tr implies tracing over coordinates as well. Explicitly,

$$G_{\varepsilon_1\varepsilon_2}(x,y)=\frac{\sinh\lambda\left(\frac{1}{2}+m\right)\sinh\lambda\left(\frac{1}{2}-M\right)}{\lambda\sinh\lambda},\tag{77}$$

where $m=\min(x,y)$, $M=\max(x,y)$, and $\lambda=\sqrt{|\varepsilon_1|+|\varepsilon_2|}$.

We start with the *weak-localization correction*. Expanding

$$\hat{V}(x)=V^0(x)+V^1(x)\hat{\Sigma}_1+V^3(x)\hat{\Sigma}_3,\tag{78}$$

with $V^i(x)$ given by Eqs. (D4)–(D6), we get the following for the expression entering Eq. (75):

$$\mathrm{Tr}\, G\hat{\Sigma}_3 V^{\chi\chi}_{\epsilon,-\epsilon}=2\int_{-1/2}^{1/2}dx\, G_{\varepsilon,-\varepsilon}(x,x)[V^3(x)]^{\chi\chi}_{\epsilon,-\epsilon}.\tag{79}$$

Evaluating the integral using Eqs. (77) and (D6), we obtain the weak-localization correction,

$$\Delta_{\mathrm{WL}}I(\chi)=-\frac{ekT}{8\hbar}\sin\chi\sum_\epsilon\frac{\Delta^2}{\epsilon^2}\frac{\cosh 2\kappa}{\sinh^3\kappa}(2\kappa-\tanh 2\kappa),\tag{80}$$

where $\kappa=\sqrt{2|\varepsilon|}=\sqrt{2|\epsilon|/E_T}$.

For short junctions ($kT_c\ll E_T$),

$$\Delta_{\mathrm{WL}}I(\chi)=-\frac{e\Delta^2}{12\hbar kT}\sin\chi,\tag{81}$$

and $\Delta_{\mathrm{WL}}I(\chi)/I(\chi)=-G_Q/3G_N$.

For long junctions ($E_T\ll kT_c$),

$$\Delta_{\mathrm{WL}}I(\chi)=-\frac{4}{\pi}\frac{e\Delta^2}{\hbar\sqrt{2\pi kTE_T}}e^{-\sqrt{2\pi kT/E_T}}\sin\chi,\tag{82}$$

and $\Delta_{\mathrm{WL}}I(\chi)/I(\chi)=-G_Q/2G_N$.

Mesoscopic fluctuations are calculated in Appendix D

with the help of Eq. (76). The result has the form

$$\langle\langle I(\chi_1)I(\chi_2)\rangle\rangle=4\left(\frac{ekT}{\hbar}\right)^2\sin\chi_1\sin\chi_2$$
$$\times\sum_{\epsilon_1\epsilon_2}\frac{\Delta^4}{\epsilon_1^2\epsilon_2^2}\left(\frac{\kappa_1}{\sinh\kappa_1}\right)^2\left(\frac{\kappa_2}{\sinh\kappa_2}\right)^2\Upsilon_{\varepsilon_1\varepsilon_2},\tag{83}$$

where the function $\Upsilon_{\varepsilon_1\varepsilon_2}$ is defined in Eq. (D10).

For short junctions ($kT_c\ll E_T$), one can take the limit $\kappa_1,\kappa_2,\lambda\to 0$ and get $\Upsilon_{\varepsilon_1\varepsilon_2}=1/30$, leading to

$$\langle\langle I(\chi_1)I(\chi_2)\rangle\rangle=\frac{1}{120}\left(\frac{e\Delta^2}{\hbar kT}\right)^2\sin\chi_1\sin\chi_2.\tag{84}$$

This result could have been deduced already from the exact result [Eq. (69)] for short junctions. The relative fluctuations of the Josephson current are $\delta I(\chi)/I(\chi)=\sqrt{2/15}G_Q/G_N$.

For long junctions ($E_T\ll kT_c$), the sums in Eq. (83) are dominated by the lowest Matsubara frequencies $\epsilon_1,\epsilon_2=\pm\pi T$ and $\Upsilon_{\pi T,\pi T}=e^{2\kappa}/128\kappa^2$, with $\kappa=\kappa_1=\kappa_2$. Hence,

$$\langle\langle I(\chi_1)I(\chi_2)\rangle\rangle=\frac{4e^2\Delta^4}{\pi^3\hbar^2kTE_T}e^{-\sqrt{8\pi kT/E_T}}\sin\chi_1\sin\chi_2,\tag{85}$$

and the relative mesoscopic fluctuations are $\delta I(\chi)/I(\chi)=G_Q/2\sqrt{2}G_N$.

3. Arbitrary wire at zero temperatures

Finally, we discuss the case of an arbitrary wire at zero temperature when the problem can be solved only numerically. Here, the amplitude of mesoscopic fluctuations, $\delta I(\chi)$, and WL correction, $\Delta_{\mathrm{WL}}I(\chi)$, are functions of two parameters: the ratio Δ/E_T and the phase difference χ.

The dependencies of the WL correction to the critical current and its mesoscopic fluctuations on Δ/E_T are presented in Figs. 11 and 12, respectively. One can clearly see the crossover from the short to long limits at $\Delta\sim 5E_T$. Note that the relative magnitude of mesoscopic fluctuations shown in Fig. 12(b) is nearly insensitive to the wire's length and can be approximated by $\delta I_c/I_c\sim 0.44G_Q/G_N$.

For long junctions ($E_T\ll\Delta$), the energy scale for mesoscopic fluctuations is set by the Thouless energy: $\delta I_c=1.490eE_T/\hbar$ and $\Delta_{\mathrm{WL}}I_c=-1.754eE_T/\hbar$. The χ dependences of the WL correction and mesoscopic fluctuations in this regime are shown in Figs. 13 and 14, respectively. These plots are inaccurate in the vicinity of $\chi=\pi$, where the Gaussian approximation breaks down (see discussion in Secs. II E and III B 1). The region of strong non-Gaussian fluctuations is specified by the inequalities

$$T\ll\delta\quad\text{and}\quad|\chi-\pi|\ll G_Q/G_N\tag{86}$$

[see Eqs. (44) and (72)]. Note that our result for the magnitude of mesoscopic fluctuations of the critical current for long wires is 2.5 times larger than the prediction of Ref. 5.

C. Interaction effects and limits of validity

Now, we briefly comment on the role of electron-electron interaction in the wire. Due to the absence of tunnel barriers,
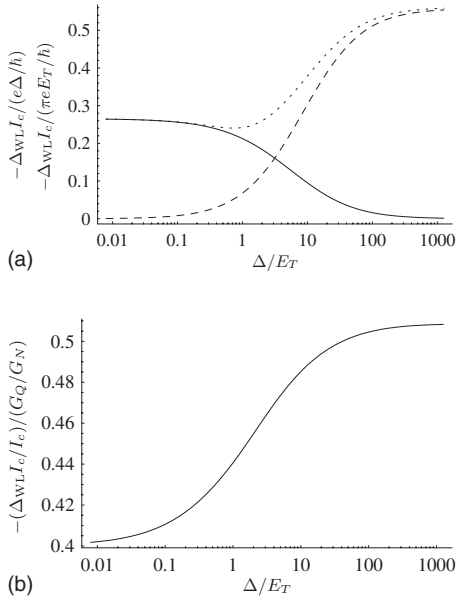
FIG. 11. (a) Weak-localization correction to the critical current $-\Delta_{\mathrm{WL}}I_c$ (solid line: in units of $e\Delta/\hbar$, dashed line: in units of $\pi eE_g/\hbar$, and dotted line: in units of $eE_*/\hbar$) vs Δ/E_T at zero temperature. (b) The ratio $-\Delta_{\mathrm{WL}}I_c/I_c$ (in units of G_Q/G_N) vs Δ/E_T at zero temperature.

the charging effects potentially relevant in the quantum dot geometry (see Sec. II F) are not important for wires, and the effect of interaction can be accounted for by the standard term in the action:[31,51]
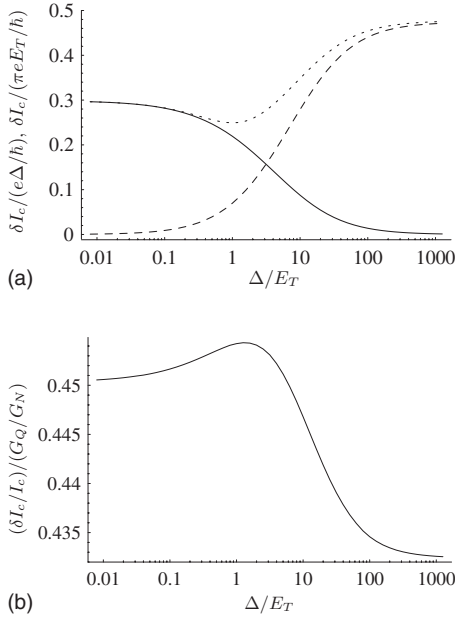

FIG. 12. (a) The amplitude of mesoscopic fluctuations of the critical current δI_c (solid line: in units of $e\Delta/\hbar$, dashed line: in units of $\pi eE_T/\hbar$, and dotted line: in units of $eE_*/\hbar$) vs Δ/E_T at zero temperature. (b) The ratio $\delta I_c/I_c$ (in units of G_Q/G_N) vs Δ/E_T at zero temperature.
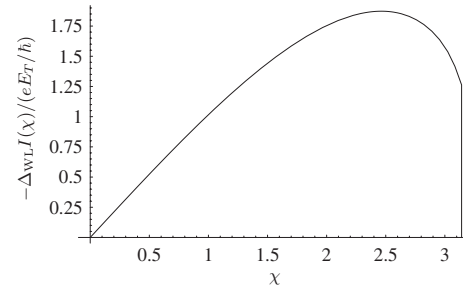

FIG. 13. Weak-localization correction $-\Delta_{\mathrm{WL}}I(\chi)$ (in units of $eE_T/\hbar$) vs χ for long wires at zero temperature.

$$S_{\mathrm{int}} = \frac{\pi^2\nu}{8}\sum_{a=1}\sum_{j=0,3}\int_0^\beta dt \int d\mathbf{r}\{\Gamma^s\,\mathrm{tr}[\,\tau_j Q_{tt}^{aa}(\mathbf{r})]^2$$
$$- \Gamma^t\,\mathrm{tr}[\,\tau_j\boldsymbol{\sigma}Q_{tt}^{aa}(\mathbf{r})]^2\}, \tag{87}$$

where Γ^s and Γ^t are the interaction amplitudes in the singlet and triplet channels, respectively. This term does not modify the average Josephson current since the corresponding correction to the Usadel equation [Eq. (50)] vanishes for the stationary (energy-diagonal) saddle-point solution $Q_0(x)$. Nor does the term [Eq. (87)] influence mesoscopic fluctuations. It follows from the fact that the interaction vertex [Eq. (87)] does not mix the replica indices and therefore cannot contribute to matrix $\hat{A}^{ab}$ [see Eq. (35)] with different replica indices $a \neq b$. This situation is completely analogous to the absence of direct Coulomb contribution to mesoscopic conductance fluctuations.[52]

Coulomb interaction indirectly influences mesoscopic effects in wires by destroying coherence at scales exceeding the phase breaking length L_ϕ. Interaction effects can be neglected as long as $L \ll L_\phi$.

Finally, we comment on the validity of the Gaussian treatment of the replicated σ model. Generally, it is controlled by the large dimensionless conductance $G_N/G_Q \gg 1$. The Gaussian approximation is violated at low temperatures in a small vicinity of $\chi = \pi$ [see Eqs. (72) and (86) for short and long wires, respectively]. Another issue is the role of instanton effects, which can be considered as saddle points of the action of Eq. (49) with a nontrivial structure in the replica space.[53] Though the instanton action is of the order of $G_N/G_Q \gg 1$, the one-dimensional geometry of the problem
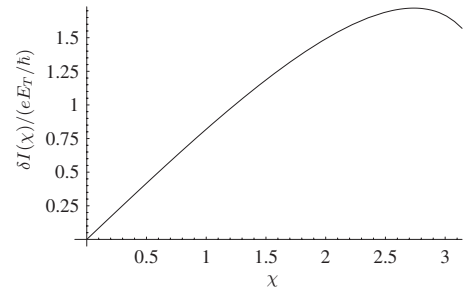

FIG. 14. Mesoscopic fluctuations $\delta I(\chi)$ (in units of $eE_T/\hbar$) vs χ for long wires at zero temperature.

TABLE II. Summary of results for a wire with conductance G_N contacted to superconducting leads. [Here, $g_N = G_N/G_Q$, $\Delta(T) = [(8\pi^2/7\zeta(3))k^2 T_c (T_c - T)]^{1/2}$, and $\mathcal{E} = \sqrt{2\pi k T E_T} \exp(\sqrt{2\pi k T/E_T})$.]

	$\chi_c/(\pi/2)$	eI_c/G_N	$\hbar\delta I_c/e$	$g_N\delta I_c/I_c$	$\hbar\Delta_{WL}I_c/e$	$g_N\Delta_{WL}I_c/I_c$
$\Delta \ll E_T$, $T=0$	1.255	2.082Δ[a]	0.30Δ[b,c]	0.45	-0.266Δ[b]	-0.401
$E_T \ll \Delta$, $T=0$	1.271	$10.83E_T$[d]	$1.490E_T$	0.432	$-1.754E_T$	-0.509
Arbitrary E_T/Δ, $T=0$	Fig. 7(a)	Fig. 7(b)[d]	Fig. 12(a)	Fig. 12(b)	Fig. 11(b)	Fig. 11(b)
$kT \lesssim kT_c \ll E_T$	1	$\pi\Delta^2(T)/4kT_c$[a]	$\Delta^2(T)/\sqrt{120kT}$	$\sqrt{2/15}$	$-\Delta^2(T)/12kT$	$-1/3$
$E_T \ll kT \lesssim kT_c$	1	$8\Delta^2(T)/\mathcal{E}$[e]	$2^{3/2}\Delta^2(T)/\pi\mathcal{E}$	$1/(2\sqrt{2})$	$-4\Delta^2(T)/\pi\mathcal{E}$	$-1/2$

[a]Reference 11.
[b]Reference 16.
[c]Reference 17.
[d]Reference 13.
[e]Reference 12.

favors proliferation of instantons due to the entropic factor. Nevertheless, we expect that these effects are irrelevant as long as the wire length is much smaller than the localization length, which gives the same condition: $G_N/G_Q \gg 1$.

D. Summary of results

The results of this section are summarized in Table II. The critical current at low temperatures is related to the minigap in the normal region at $\chi=0$, $E_* \sim \min(E_T, \Delta)$, through an Ambegaokar-Baratoff-like formula: $I_c \sim G_N E_*/e$. We see that, quite generally, mesoscopic fluctuations and WL correction to the Josephson current are suppressed by the factor G_Q/G_N: $\delta I_c \sim -\Delta_{WL}I_c \sim eE_*/\hbar$, where the precise coefficients in this expression depend on the wire's length and temperature. Note that contrary to the S-QD-S cases considered in Sec. II, these coefficients are always of the order of 1. This should be compared to the behavior of the conductance. In a normal metallic wire, conductance fluctuations and its weak-localization correction are also suppressed by the same factor G_Q/G_N, but the coefficients are "universal:" $\delta G_N = \sqrt{2/15}G_Q$ and $\Delta_{WL}G_N = -G_Q/3$. Note that for short wires at T close to T_c, the relative WL correction and mesoscopic fluctuations of I_c coincide with those of the conductance. This is due to the relation $I(\chi) \propto G \sin\chi$, see discussion in the end of Sec. II G.

IV. MESOSCOPIC FLUCTUATIONS IN TWO-DIMENSIONAL AND THREE-DIMENSIONAL GEOMETRIES

A. Mesoscopic fluctuations of the Josephson current through a two-dimensional electron gas

In Ref. 23, mesoscopic fluctuations of the critical current had been measured in junctions formed by a two-dimensional electron gas whose width W was much longer than the distance L between the superconducting electrodes. In this case, the results of Sec. III cannot be applied since transverse diffusive modes become relevant. In this section, we take them into account and calculate rms δI_c for the two-dimensional geometry.

Mesoscopic fluctuations can be obtained with the help of the general formula [Eq. (39)], where now the operator $\hat{A}$ reads

$$\hat{A}^{(2D)}(x,y) = -\frac{\partial^2}{\partial y^2} + \hat{A}(x). \quad (88)$$

Here, $\hat{A}(x)$ stands for operator (65) for the quasi-one-dimensional wire, and $-1/2 < x < 1/2$ ($0 < y < W/L$) is the dimensionless coordinate along (perpendicular to) the junction.

The eigenvalues of operator (88) are given by

$$\lambda_{m,i} = \frac{\pi^2 m^2}{\eta^2} + \lambda_i, \quad (89)$$

where $\eta = W/L$, and λ_i are the eigenvalues of the operator $\hat{A}(x)$ (we suppressed the indices χ_1, χ_2 and $\varepsilon, \varepsilon'$ for brevity). For wires, only the zeroth transverse diffusive mode with $m=0$ was relevant, whereas for the film geometry, one has to sum over all m's. As a result, we can express the current cumulant in terms of the spectrum of the operator $\hat{A}(x)$,

$$\langle\langle I(\chi_1)I(\chi_2)\rangle\rangle = -8\left(\frac{ekT}{\hbar}\right)^2 \frac{\partial^2}{\partial\chi_1\partial\chi_2} \sum_{\varepsilon\varepsilon'} \text{tr } F(A_{\varepsilon\varepsilon'}^{\chi_1\chi_2}), \quad (90)$$

where

$$F(\lambda) = \ln\left(\frac{\sqrt{\lambda}}{\eta} \sinh\eta\sqrt{\lambda}\right) \quad (91)$$

is a generalization of the function $\ln\lambda$ relevant for wires to arbitrary ratios $\eta = W/L$.

We analyze Eqs. (90) and (91) in the experimentally relevant limit[23] of wide ($W \gg L$) and long ($E_T \equiv \hbar D/L^2 \ll \Delta$) junctions, at small temperatures ($kT \ll E_T$). Then, $F(\lambda) \approx \eta\sqrt{\lambda}$, and the spectral sum should be calculated numerically, analogously to the quasi-one-dimensional situation (see Sec. III B 3). We obtain the following for the rms of the critical current fluctuations (at $\chi_c = 1.27\pi/2$):

$$\delta I_c = 1.5\frac{eE_T}{\hbar}\sqrt{\frac{W}{L}}. \quad (92)$$

A similar equation with the prefactor 2.2 was used in Ref. 23 [see Eq. (2) there] as the theoretical estimate for the critical current fluctuations. Though the two-dimensional case was not considered by Altshuler and Spivak,[5] it was claimed that Eq. (2) of Ref. 23 can be obtained from the three-dimensional result of Ref. 5. We could not follow the derivation of Eq. (2) in Ref. 23 but would like to emphasize that even the three-dimensional result for δI_c from Ref. 5 is overestimated in Eq. (1) of Ref. 23 by the factor of π^2 due a different definition of the Thouless energy. So, we expect that the 2D result for δI_c obtained within the Altshuler-Spivak approach would have the form of Eq. (92), with the prefactor smaller than 1.

Thus, even though the approach of Ref. 5 generally underestimates the magnitude of critical current fluctuations, the theoretical prediction of Ref. 23 overestimated them by a factor of 1.5.

For completeness, we present also the result for wide ($W \gg L$) and short ($\Delta \ll E_T$) junctions at $T=0$. It can be obtained using the spectrum found in Sec. III B 1. We get the following for the rms of the critical current fluctuations:

$$\delta I_c = 0.26 \frac{e\Delta}{\hbar} \sqrt{\frac{W}{L}}. \tag{93}$$

B. Three-dimensional case

Finally, we mention that the above results for the 2D case can be easily generalized to the 3D case. To be specific, we consider the limit of wide junctions when both transverse dimensions are large: $W_y, W_z \gg L$. Then, mesoscopic fluctuations can be found with the help of Eq. (90) with $F(\lambda) = (W_y W_z / 4\pi L^2)\lambda \ln M/\lambda$, where $M \sim L/l$ is the high-momentum cutoff [it drops from the answer since $\partial^2 \operatorname{tr} \hat{A} / \partial\chi\partial\chi' = 0$: see Eq. (65)].

For long junctions ($E_T \ll \Delta$) at $T=0$, a numerical integration leads to Eq. (3). Note that the result of Ref. 5 obtained in the same limit contains the numerical factor $\sqrt{15\zeta(5)/\pi^3} = 0.71$ instead of 2.0. Again, we see that the approach of Ref. 5 underestimates the magnitude of mesoscopic fluctuations of I_c by a factor of 2.8. For short junctions ($\Delta \ll E_T$) at $T=0$, we obtain

$$\delta I_c = 0.28 \frac{e\Delta}{\hbar} \sqrt{\frac{W_y W_z}{L^2}}. \tag{94}$$

V. COMPARISON WITH EXPERIMENTS

In metals, the mesoscopic fluctuations of the conductance are usually measured by varying a small magnetic field applied to the sample. When the leads connecting the sample are superconducting, the Josephson effect may take place. However, the characteristic field for the conductance variations in normal state coincides with the field above which the Josephson effect is suppressed in the superconducting state. This precludes the observation of mesoscopic fluctuations of the Josephson supercurrent by this method.

Alternatively, the mesoscopic fluctuations were obtained by measuring the conductance after successive annealings of the sample[54] or by recording the $1/f$ noise in the conductance fluctuations (see Feng and Giordano in Ref. 4). In the first case, the impurity configuration is effectively changed at each thermal cycle. In the second one, the low frequency noise is attributed to slow displacements of single defects, with a strong effect on the interference contribution to the conductance.[55,56] We are not aware of any attempt to measure the mesoscopic fluctuations of the Josephson current following these methods.

In semiconductors, the large field effect allows us to change effectively the impurity configuration by applying an external gate voltage. Mesoscopic fluctuations were obtained this way in Refs. 23 and 24. In Ref. 23, mesoscopic fluctuations of I_c were studied in a geometry of a wide ($W \gg L$), long ($E_T \ll \Delta$) bar of a two-dimensional electron gas. Experimentally, the observed fluctuation magnitude (in the weakly localized regime I) is three times smaller than our result [Eq. (92)]: $\delta I_c^{\text{theor}} = 45$ nA, $\delta I_c^{\text{expt}} = 15$ nA. The discrepancy might be attributed either to nonideal transparencies of the NS interfaces leading to charging effects discussed in Sec. II F or to fluctuations in the superconducting phase due to the electromagnetic environment in which the junction is embedded.

The experiment of Ref. 24 refers to the quasi-one-dimensional short ($\Delta \ll E_T$) wires and should be compared with the result[16,17] $\delta I_c = 0.30 e\Delta/\hbar$. Again the theoretical prediction (~ 10 nA with $\Delta = 0.155$ meV) appears to be several times larger than the experimentally measured magnitude (< 2 nA). However, the assumption of short wire is questionable: The amplitude of the critical current as well as its temperature dependence are rather suggestive of a ratio $\Delta/E_T \gtrsim 10$ in the samples of Ref. 24. The Thouless energy may have been overestimated by taking the spatial gap between the superconducting electrodes as the junction length. Instead, nonideal transparencies of the contact between the wire and the superconducting leads may result in an effectively increased junction length. On the other hand, we note that the ratio $G_N \delta I_c / G_Q I_c$ is predicted to be almost constant for junctions of arbitrary length [see Fig. 12(b)]. This is in reasonable agreement with what was found experimentally.

VI. CONCLUSION

In this work, we used the replica σ-model technique to describe mesoscopic fluctuations and weak-localization correction to the equilibrium supercurrent in Josephson junctions formed of a metallic wire between superconducting leads. We considered two types of junctions: a chaotic dot coupled to superconductors by tunnel barriers (S-QD-S) and a diffusive wire (SNS) with transparent NS interfaces. In both cases, we calculated the amplitude of supercurrent fluctuations and the weak-localization correction to the average current $I(\chi)$ in different temperature regions at arbitrary ratios between Δ and E_{dwell} (given by E_g for an S-QD-S junction and by E_T for an SNS junction).

For a quasi-one-dimensional SNS junction, we have found that mesoscopic corrections to the quasiclassical Josephson current are "nearly universal:" $\delta I_c / I_c \sim -\Delta_{\text{WL}} I_c / I_c$

$\sim G_Q/G$, where the exact coefficients in these relations are of the order of 1, being slightly dependent on the parameters of the junction. For a double-barrier S-QD-S junction, the weak-localization correction vanishes, while mesoscopic fluctuations are "less universal:" $\delta I_c/I_c \sim G_Q/G$ for junctions with $kT_c \ll E_g$ and is additionally suppressed for junctions with $E_g \ll kT_c$.

We also demonstrated that the approach of Ref. 5 systematically underestimates the magnitude of mesoscopic fluctuations of the critical current by factors around 2.5–2.8, both in the quasi-one-dimensional and three-dimensional cases.

We compared our predictions with the experimental results obtained for a wide $(W \gg L)$, long $(E_T \ll \Delta)$ bar of a two-dimensional electron gas[23] and for a quasi-one-dimensional, short $(\Delta \ll E_T)$ wire.[24] In both cases, the theory predicts a larger mesoscopic fluctuation of the critical current than what was measured. We pointed out the nonideal transparencies of the NS contacts and the fluctuation of the superconducting phase across the junction due to its electromagnetic environment as possible sources of the discrepancy.

Among the motivations to study mesoscopic fluctuations, it was suggested that they may induce the sign change of the critical current (π-junction behavior).[57] However, such possibility was discarded in Ref. 58 if time-reversal symmetry is preserved in the normal part and if interactions are absent. If the normal part is ferromagnetic, time-reversal symmetry is broken. Then, with strong barriers between the wire and leads, it was shown that mesoscopic fluctuations are dominant in the Josephson relation compared to the quasiclassical contribution.[59] Within our approach, this study could be easily reconsidered and extended by adding an exchange energy term in the Hamiltonian of the wire. We note that the replica σ model is also appropriate for taking electron-electron interactions into account. This could be the subject of future studies.

APPENDIX A: SOLUTION OF THE USADEL EQUATIONS FOR A WIRE

1. Determination of the spectral current J and $\theta(0)$

For a fixed $\varepsilon > 0$, θ_s and χ, the values of the spectral current J and the Usadel angle $\theta_0 \equiv \theta(0)$ in the middle of the wire are determined from two equations,

$$\sqrt{\varepsilon} = \int_{\theta_0}^{\theta_s} \frac{d\theta}{\mathcal{R}(\theta)}, \tag{A1a}$$

$$\chi = 2\sqrt{\alpha} \int_{\theta_0}^{\theta_s} \frac{1}{\sin^2 \theta} \frac{d\theta}{\mathcal{R}(\theta)}, \tag{A1b}$$

where $\mathcal{R}(\theta) = [\cos \theta_0 - \cos \theta + \alpha(\sin^{-2} \theta_0 - \sin^{-2} \theta)]^{1/2}$ and $\alpha = J^2/4\varepsilon$. These integrals can be converted to the standard elliptic integrals,

$$\sqrt{\varepsilon} = \frac{2F(\varphi, k)}{\sqrt{a - c}}, \tag{A2a}$$

$$\chi = \frac{4\sqrt{\alpha} F(\varphi, k)}{(1 - a^2)\sqrt{a - c}} + \frac{2\sqrt{\alpha}(b - a)}{\sqrt{a - c}} \left[\frac{\Pi\left(\varphi, k^2 \frac{1 - a}{1 - b}, k\right)}{(1 - a)(1 - b)} - \frac{\Pi\left(\varphi, k^2 \frac{1 + a}{1 + b}, k\right)}{(1 + a)(1 + b)} \right], \tag{A2b}$$

where

$$\begin{Bmatrix} a \\ c \end{Bmatrix} = \frac{\alpha}{2 \sin^2 \theta_0} \pm \sqrt{1 + \frac{\alpha \cos \theta_0}{\sin^2 \theta_0} + \frac{\alpha^2}{4 \sin^4 \theta_0}}, \tag{A3a}$$

$$b = \cos \theta_0, \quad k = \sqrt{\frac{b - c}{a - c}}, \tag{A3b}$$

$$\varphi = \arcsin \sqrt{\frac{(a - c)(b - \cos \theta_s)}{(b - c)(a - \cos \theta_s)}}. \tag{A3c}$$

Note that our definition of elliptic integrals $F(\varphi, k)$ and $\Pi(\varphi, n, k)$ coincides with that of Ref. 34. The same functions are often defined in a different way:[60] in MATHEMATICA, e.g.,

$$F(\varphi, k) = \texttt{EllipticF}[\varphi, k^2]$$

and

$$\Pi(\varphi, n, k) = \texttt{EllipticPi}[n, \varphi, k^2].$$

Equations (A2a) and (A2b) should be solved numerically to obtain α and b (and hence J and θ_0) for given $\varepsilon > 0$, θ_s, and χ. The Usadel angles for $\varepsilon < 0$ can be obtained from Eqs. (52).

2. Determination of $\theta(x)$ and $\eta(x)$

For each ε, we first have to find θ_0 and α as described above. Then, for a spatial point x_i, the value $\theta_i = \theta(x_i)$ can be found from the equation

$$|x_i| = \frac{F(\varphi_i, k)}{\sqrt{\varepsilon}\sqrt{a - c}}, \quad \varphi_i = \arcsin \sqrt{\frac{(a - c)(b - \cos \theta_i)}{(b - c)(a - \cos \theta_i)}}, \tag{A4}$$

which can be solved as

$$\cos \theta_i = \frac{b - aY}{1 - Y}, \quad Y = \frac{b - c}{a - c} sn^2[|x_i|\sqrt{\varepsilon(a - c)}, k], \quad \text{(A5)}$$

where $sn(u, k)$ is the Jacobi elliptic function.[34] In MATHEMATICA, e.g., $sn(u, k) = \texttt{JacobiSN}[u, k^2]$.

Then, we determine $\eta_i = \eta(x_i)$ from Eq. (68),

$$\eta_i = -\frac{\sqrt{\alpha}}{2} \int_{\theta_0}^{\theta_i} \frac{1}{(\cos \theta_0 - \cos \theta) + \frac{\alpha}{\sin^2 \theta_0}} \frac{d\theta}{\mathcal{R}(\theta)}. \quad \text{(A6)}$$

Converting this to elliptic integrals and using Eq. (A4), we get

$$\eta_i = -\frac{\sqrt{\varepsilon \alpha} x_i}{(p - a)} - \frac{x_i}{|x_i|} \frac{\sqrt{\alpha(b - a)}}{\sqrt{a - c}} \frac{\Pi\left(\varphi_i, k^2 \frac{p - a}{p - b}, k\right)}{(p - a)(p - b)}, \quad \text{(A7)}$$

where $p = \cos \theta_0 + \alpha / \sin^2 \theta_0$. Note that $\eta(x)$ is an odd function of x.

The functional determinants of $\hat{A}(x)$ involved in Eqs. (34) and (39) can be calculated numerically by introducing a proper grid x_i. Then, we discretize the Laplace operator in the operator $\hat{A}$ [Eq. (65)] and find α_{mn}, ρ_{mn}, η_m, and η_n for each x_i, thus defining a finite matrix $\hat{A}_{ij}$. The functional determinants in Eqs. (34) and (39) can then be approximated by determinants of the matrix $\hat{A}_{ij}$, which should be evaluated numerically.

APPENDIX B: DERIVATION OF THE OPERATOR A FOR A WIRE

Substituting Eq. (22) into Eq. (49) and expanding the action to the second order in W, we get

$$S^{(2)} = \frac{G_N}{16 G_Q} \int_{-1/2}^{1/2} dx \operatorname{tr}[-(\nabla W)^2 + \{\mathcal{J}, W\}^2 - 2\mathcal{J}\tau_1[W, \nabla W]$$
$$- 2\varepsilon U \tau_3 U^\dagger \tau_1 W^2], \quad \text{(B1)}$$

where $\mathcal{J} = U \nabla U^\dagger \tau_1$. Using the decomposition [Eq. (26)] of W in terms of the d and c modes, we rewrite $S^{(2)}$ in the form of Eq. (64), where

$$\hat{A}_{mn}(x) = -\nabla^2 + \alpha_{mn} + \lambda_{mn}^2/4 - i\hat{\Sigma}_2[\lambda_{mn}\nabla + (\nabla\lambda_{mn})/2]$$
$$+ \beta_{mn}\hat{\Sigma}_3 + \gamma_{mn}\hat{\Sigma}_1. \quad \text{(B2)}$$

Here, $m = (\varepsilon, a)$ and $n = (\varepsilon', b)$ are energy and replica indices, $\hat{\Sigma}_{i=1,2,3}$ are the Pauli matrices in the (d, c) space, α_{mn} is given by Eq. (66), and

$$\lambda_{mn} = -(\cos \theta_n \nabla \phi_n + \cos \theta_m \nabla \phi_m), \quad \text{(B3a)}$$

$$\beta_{mn} = (\sin \theta_n \nabla \phi_n \sin \theta_m \nabla \phi_m - \nabla \theta_n \nabla \theta_m)/2, \quad \text{(B3b)}$$

$$\gamma_{mn} = -(\sin \theta_n \nabla \phi_n \nabla \theta_m + \sin \theta_m \nabla \phi_m \nabla \theta_n)/2. \quad \text{(B3c)}$$

Here, (θ_m, ϕ_m) and (θ_n, ϕ_n) are the solutions of the Usadel equations [Eqs. (51a) and (51b)] at energies ε and ε', and phase difference χ_1 or χ_2, depending on the replica indices a and b, respectively.

In order to remove the first order derivative in Eq. (B2), we make a local unitary transformation in the (d, c) space: $(d, c)_{mn}^T \to \mathcal{V}_{mn}(d, c)_{mn}^T$, where

$$\mathcal{V}_{mn} = \cos \frac{\zeta_n + \zeta_m}{2} - i\hat{\Sigma}_2 \sin \frac{\zeta_n + \zeta_m}{2}, \quad \text{(B4a)}$$

$$\zeta_m(x) = -\int_0^x ds \cos \theta_m(s) \nabla \phi_m(s). \quad \text{(B4b)}$$

Such a rotation leaves $\det \hat{A}$ and $A_{\varepsilon, -\varepsilon}^{\chi\chi}$ invariant, while the operator $\hat{A}$ is transformed to

$$\hat{\tilde{A}} = \mathcal{V}_{mn}^\dagger \hat{A}_{mn} \mathcal{V}_{mn}, \quad \text{(B5)}$$

which can be written in the form of Eq. (65) (tilde omitted) with

$$\eta_m = -\arctan \frac{\nabla \theta_m}{\sin \theta_m \nabla \phi_m} - \zeta_m. \quad \text{(B6)}$$

Taking the derivative of Eq. (B6), we come to Eq. (68).

APPENDIX C: EQUIVALENCE OF EQUATION (69) TO THE RESULTS OF REFERENCES 16 and 17

The result for the variance of the Josephson current, $\operatorname{var} I(\chi) = \delta I^2(\chi)$, obtained in Refs. 16 and 17 can be written in the form

$$\operatorname{var} I(\chi) = \frac{1}{2}\left(\frac{e\Delta}{\pi\hbar}\right)^2 \int_0^\infty dk k(1 - e^{-\pi k})|a(k)|^2, \quad \text{(C1)}$$

$$a(k) = \int_0^\infty \frac{dx \cos kx \sin \chi}{\cosh x \sqrt{\cosh^2 x - \sin^2 \frac{\chi}{2}}}. \quad \text{(C2)}$$

In this appendix, we show that our expression [Eq. (69)] for $\langle\langle I(\chi) I(\chi') \rangle\rangle$ at $\chi' = \chi$ and zero temperature gives the same result. We start with rewriting Eq. (69) in the form of integrals over C and C',

$$\operatorname{var} I(\chi) = -\frac{1}{2}\left(\frac{e\Delta}{\pi\hbar}\right)^2 \int_0^{\chi/2} \frac{dC \sin \chi}{\sin C \sqrt{\sin^2 \frac{\chi}{2} - \sin^2 C}} \frac{dC' \sin \chi}{\sin C' \sqrt{\sin^2 \frac{\chi}{2} - \sin^2 C'}} \frac{\partial^2}{\partial C \partial C'} \ln \frac{\sin(C - C')}{C - C'} \frac{\sin(C + C')}{C + C'}. \quad \text{(C3)}$$

Using Eqs. (2.29) and (3.6) from Ref. 16, we rewrite the second derivative of the logarithm as

$$\frac{\partial^2}{\partial C \partial C'} \ln \frac{\sin(C - C')}{C - C'} \frac{\sin(C + C')}{C + C'}$$

$$= -4 \int_0^\infty dk \frac{k \sinh kC \sinh kC'}{e^{\pi k} - 1}, \qquad (C4)$$

which allows us to present Eq. (C3) in the form of Eq. (C1) with $\tilde{a}(k)$ instead of $a(k)$,

$$\tilde{a}(k) = \frac{1}{\sinh(\pi k/2)} \int_0^{\chi/2} \frac{dC \sinh kC \sin \chi}{\sin C \sqrt{\sin^2 \frac{\chi}{2} - \sin^2 C}}. \quad (C5)$$

The equivalence between our result and the result of Refs. 16 and 17 follows from the equality $a(k) = \tilde{a}(k)$. To prove it, we extend the integration in Eq. (C2) to the real axis, substituting $\cos kx$ by e^{ikx}. Then, we deform the integration contour to the upper half-plane and enclose all branch cuts of the square root: $[i(\pi n + \pi/2 - \chi/2), i(\pi n + \pi/2 + \chi/2)]$, $n = 0, 1, \ldots$. As a result, the summation of $e^{-(n+1/2)\pi k}$ over n yields $\sinh(\pi k/2)$ in the denominator, while the integration along the branch cut reproduces the integral in Eq. (C5). Thus, $a(k) = \tilde{a}(k)$, which establishes the equivalence between the two results.

APPENDIX D: SOLUTION OF THE USADEL EQUATION FOR A WIRE CLOSE TO T_c

Close to T_c, the solution of the Usadel equation [Eqs. (51a) and (51b)] is given by Eq. (60). It corresponds to the following dependence of $\theta(x)$ and $\phi(x)$:

$$\sin \theta(x) = \frac{\sin \theta_s}{\sinh \kappa}$$

$$\times \sqrt{\cosh 2\kappa x (\cosh \kappa - \cos \chi) - (1 - \cosh \kappa \cos \chi)}, \qquad (D1)$$

$$\tan \phi(x) = \frac{\tan \frac{\chi}{2}}{\tanh \frac{\kappa}{2}} \tanh \kappa x \qquad (D2)$$

(this form is valid for both $\varepsilon > 0$ and $\varepsilon < 0$). The function $\eta(x)$ defined in Eq. (68) is given by

$$\tan \eta(x) = -\operatorname{sgn}(\varepsilon) \frac{\tanh \frac{\kappa}{2}}{\tan \frac{\chi}{2}} \tanh \kappa x. \qquad (D3)$$

The rigidity of Gaussian fluctuations near the saddle point is determined by the operator $\hat{A}_{\varepsilon_1 \varepsilon_2} = -\nabla^2 + |\varepsilon_1| + |\varepsilon_2| + \hat{V}_{\varepsilon_1 \varepsilon_2}$, where the operator $\hat{V}$ can be expanded in the Pauli matrices [Eq. (78)] with the coefficients

$$V^0(x) = -\frac{1}{2} \left(\frac{\Delta}{|\epsilon_1|} \frac{\kappa_1}{\sinh \kappa_1} \right)^2 (\cosh \kappa_1 - \cos \chi_1) \cosh 2\kappa_1 x$$

$$- \frac{1}{2} \left(\frac{\Delta}{|\epsilon_2|} \frac{\kappa_2}{\sinh \kappa_2} \right)^2 (\cosh \kappa_2 - \cos \chi_2) \cosh 2\kappa_2 x, \qquad (D4)$$

$$V^1(x) = -2 \frac{\Delta}{|\epsilon_1|} \frac{\kappa_1}{\sinh \kappa_1} \frac{\Delta}{|\epsilon_2|} \frac{\kappa_2}{\sinh \kappa_2} \left(\operatorname{sgn}(\varepsilon_1) \cos \frac{\chi_1}{2} \sin \frac{\chi_2}{2} \sinh \frac{\kappa_1}{2} \cosh \frac{\kappa_2}{2} \sinh \kappa_1 x \cosh \kappa_2 x \right.$$

$$\left. + \operatorname{sgn}(\varepsilon_2) \sin \frac{\chi_1}{2} \cos \frac{\chi_2}{2} \cosh \frac{\kappa_1}{2} \sinh \frac{\kappa_2}{2} \cosh \kappa_1 x \sinh \kappa_2 x \right), \qquad (D5)$$

$$V^3(x) = 2 \frac{\Delta}{|\epsilon_1|} \frac{\kappa_1}{\sinh \kappa_1} \frac{\Delta}{|\epsilon_2|} \frac{\kappa_2}{\sinh \kappa_2} \left(\sin \frac{\chi_1}{2} \sin \frac{\chi_2}{2} \cosh \frac{\kappa_1}{2} \cosh \frac{\kappa_2}{2} \cosh \kappa_1 x \cosh \kappa_2 x \right.$$

$$\left. - \operatorname{sgn}(\varepsilon_1 \varepsilon_2) \cos \frac{\chi_1}{2} \cos \frac{\chi_2}{2} \sinh \frac{\kappa_1}{2} \sinh \frac{\kappa_2}{2} \sinh \kappa_1 x \sinh \kappa_2 x \right). \qquad (D6)$$

The supercurrent correlation function [Eq. (76)] involves

$$R_{\varepsilon_1 \varepsilon_2} = \operatorname{Tr}(G\hat{V})^2 = 2 \int_{-1/2}^{1/2} dx dy G_{\varepsilon_1 \varepsilon_2}^2(x, y) \sum_{i=0,1,3} V^i(x) V^i(y). \qquad (D7)$$

Since current fluctuations are determined by $\Sigma_{\varepsilon_1, \varepsilon_2} R_{\varepsilon_1 \varepsilon_2}$, it is convenient to symmetrize R by introducing

$$\tilde{R}_{\varepsilon_1, \varepsilon_2} = \frac{1}{4} [R_{\varepsilon_1, \varepsilon_2} + R_{-\varepsilon_1, \varepsilon_2} + R_{\varepsilon_1, -\varepsilon_2} + R_{-\varepsilon_1, -\varepsilon_2}], \qquad (D8)$$

such that $\Sigma_{\varepsilon_1, \varepsilon_2} R_{\varepsilon_1 \varepsilon_2} = \Sigma_{\varepsilon_1, \varepsilon_2} \tilde{R}_{\varepsilon_1 \varepsilon_2}$.

Substituting Eqs. (D4)–(D6) into Eq. (D7) and taking the derivatives with respect to χ_1 and χ_2, we get

$$\frac{\partial^2}{\partial\chi_1\partial\chi_2}\widetilde{R}_{\varepsilon_1\varepsilon_2} = \left(\frac{\Delta}{|\epsilon_1|}\frac{\kappa_1}{\sinh\kappa_1}\right)^2\left(\frac{\Delta}{|\epsilon_2|}\frac{\kappa_2}{\sinh\kappa_2}\right)^2 \Upsilon_{\varepsilon_1\varepsilon_2}\sin\chi_1\sin\chi_2, \tag{D9}$$

resulting in Eq. (83). Here, the function $\Upsilon_{\varepsilon_1\varepsilon_2}$ is defined by the double integral,

$$\Upsilon_{\varepsilon_1\varepsilon_2} = \int_{-1/2}^{1/2} dxdy\, G_{\varepsilon_1\varepsilon_2}(x,y)^2\left[\cosh 2\kappa_1 x\cosh 2\kappa_2 y + 2\cosh^2\frac{\kappa_1}{2}\cosh^2\frac{\kappa_2}{2}\cosh\kappa_1 x\cosh\kappa_2 x\cosh\kappa_1 y\cosh\kappa_2 y\right.$$

$$+ 2\sinh^2\frac{\kappa_1}{2}\sinh^2\frac{\kappa_2}{2}\sinh\kappa_1 x\sinh\kappa_2 x\sinh\kappa_1 y\sinh\kappa_2 y - 2\cosh^2\frac{\kappa_1}{2}\sinh^2\frac{\kappa_2}{2}\cosh\kappa_1 x\sinh\kappa_2 x\cosh\kappa_1 y\sinh\kappa_2 y$$

$$\left. - 2\sinh^2\frac{\kappa_1}{2}\cosh^2\frac{\kappa_2}{2}\sinh\kappa_1 x\cosh\kappa_2 x\sinh\kappa_1 y\cosh\kappa_2 y\right]. \tag{D10}$$

In principle, these integrals can be calculated in a closed form. However, the resulting expression is too complicated, and we leave the integrals unevaluated.

---

[1] E. Abrahams, P. W. Anderson, D. C. Licciardello, and T. V. Ramakrishnan, Phys. Rev. Lett. **42**, 673 (1979); L. P. Gor'kov, A. I. Larkin, and D. E. Khmel'nitskii, Pis'ma Zh. Eksp. Teor. Fiz. **30**, 248 (1979) [JETP Lett. **30**, 228 (1979)].

[2] B. L. Althsuler, Pis'ma Zh. Eksp. Teor. Fiz. **51**, 530 (1985) [JETP Lett. **41**, 648 (1985)]; P. A. Lee and A. D. Stone, Phys. Rev. Lett. **55**, 1622 (1985).

[3] S. Washburn and R. A. Webb, Adv. Phys. **35**, 375 (1986).

[4] *Mesoscopic Phenomena in Solids*, Modern Problems in Condensed Matter Sciences Vol. 30, edited by B. L. Altshuler, P. A. Lee, and R. A. Webb (North-Holland, Austerdam, 1991).

[5] B. L. Altshuler and B. Z. Spivak, Zh. Eksp. Teor. Fiz. **92**, 607 (1987) [Sov. Phys. JETP **65**, 343 (1987)].

[6] A. F. Andreev, Zh. Eksp. Teor. Fiz. **46**, 1823 (1964) [Sov. Phys. JETP **19**, 1228 (1964)].

[7] B. Z. Spivak and D. E. Khmel'nitskii, Pis'ma Zh. Eksp. Teor. Fiz. **35**, 334 (1982) [JETP Lett. **35**, 412 (1982)].

[8] W. L. McMillan, Phys. Rev. **175**, 537 (1968); A. A. Golubov and M. Yu. Kupriyanov, Zh. Eksp. Teor. Fiz. **96**, 1420 (1989) [Sov. Phys. JETP **69**, 805 (1989)]; J. A. Melsen, P. W. Brouwer, K. M. Frahm, and C. W. J. Beenakker, Europhys. Lett. **35**, 7 (1996); Phys. Scr. **69**, 223 (1997).

[9] K. D. Usadel, Phys. Rev. Lett. **25**, 507 (1970).

[10] For this reason, the theory of Ref. 5 does not allow determining correctly the average Josephson current.

[11] I. O. Kulik and A. M. Omelyanchuk, Zh. Eksp. Teor. Fiz. Pis'ma Red. **21**, 216 (1975) [JETP Lett. **21**, 96 (1975)].

[12] A. D. Zaikin and G. F. Zharkov, Fiz. Nizk. Temp. **7**, 375 (1981) [Sov. J. Low Temp. Phys. **7**, 184 (1981)].

[13] P. Dubos, H. Courtois, B. Pannetier, F. K. Wilhelm, A. D. Zaikin, and G. Schön, Phys. Rev. B **63**, 064502 (2001).

[14] A. A. Golubov, M. Yu. Kupriyanov, and E. Il'ichev, Rev. Mod. Phys. **76**, 411 (2004).

[15] C. W. J. Beenakker, Rev. Mod. Phys. **69**, 731 (1997).

[16] A. M. S. Macêdo and J. T. Chalker, Phys. Rev. B **49**, 4695 (1994).

[17] C. W. J. Beenakker and B. Rajaei, Phys. Rev. B **49**, 7499 (1994).

[18] C. W. J. Beenakker, Phys. Rev. Lett. **67**, 3836 (1991); C. W. J. Beenakker, *ibid.* **68**, 1442(E) (1992).

[19] Y. Takane, J. Phys. Soc. Jpn. **63**, 2668 (1994); A. Furusaki, Physica B **203**, 214 (1994).

[20] T. Micklitz, Phys. Rev. B **75**, 144509 (2007).

[21] K. B. Efetov, *Supersymmetry in Disorder and Chaos* (Cambridge University Press, New York, 1997).

[22] A. Altland, B. D. Simons, and D. Taras-Semchuk, Pis'ma Zh. Eksp. Teor. Fiz. **67**, 21 (1998) [JETP Lett. **67**, 22 (1998)]; Adv. Phys. **49**, 321 (2000).

[23] H. Takayanagi, J. B. Hansen, and J. Nitta, Phys. Rev. Lett. **74**, 166 (1995).

[24] Y.-J. Doh, J. A. van Dam, A. L. Roest, E. P. A. M. Bakkers, L. P. Kouwenhoven, and S. De Franceschi, Science **309**, 272 (2005).

[25] I. G. Aslamazov, A. I. Larkin, and Yu. N. Ovchinnikov, Zh. Eksp. Teor. Fiz. **55**, 323 (1968) [Sov. Phys. JETP **28**, 171 (1969)].

[26] M. Yu. Kupriyanov and V. F. Lukichev, Zh. Eksp. Teor. Fiz. **94**, 139 (1988) [Sov. Phys. JETP **67**, 1163 (1988)].

[27] P. W. Brouwer and C. W. J. Beenakker, Chaos, Solitons Fractals **8**, 1249 (1997).

[28] S. F. Edwards and P. W. Anderson, J. Phys. F: Met. Phys. **5**, 965 (1975).

[29] F. J. Wegner, Z. Phys. B **35**, 207 (1979).

[30] K. B. Efetov, A. I. Larkin, and D. E. Khmelnitskii, Zh. Eksp. Teor. Fiz. **79**, 1120 (1980) [Sov. Phys. JETP **52**, 568 (1980)].

[31] A. M. Finkel'stein, *Electron Liquid in Disordered Conductors*, Soviet Scientific Reviews Vol. 14, edited by I. M. Khalatnikov (Harwood Academic, London, 1990).

[32] Y. Oreg, P. W. Brouwer, B. D. Simons, and A. Altland, Phys. Rev. Lett. **82**, 1269 (1999).

[33] Yu. V. Nazarov, Phys. Rev. Lett. **73**, 1420 (1994).

[34] I. S. Gradshteyn and I. M. Ryzhik, *Table of Integrals, Series, and Products* (Academic, New York, 2000).

[35] P. M. Ostrovsky and M. V. Feigel'man, Pis'ma Zh. Eksp. Teor. Fiz. **82**, 863 (2005) [JETP Lett. **82**, 763 (2005)].

[36] S. Iida, H. A. Weidenmüller, and J. A. Zuk, Ann. Phys. (N.Y.) **200**, 219 (1990).

[37] J. A. Melsen and C. W. J. Beenakker, Phys. Rev. B **51**, 14483 (1995).

[38] G. Campagnano and Yu. V. Nazarov, Phys. Rev. B **74**, 125307 (2006).

[39] R. S. Whitney, Phys. Rev. B **75**, 235404 (2007).

[40] C. W. J. Beenakker, Phys. Rev. B **47**, 15763 (1993).

[41] M. Houzet and L. I. Glazman (unpublished).

[42] Y. Shimizu, H. Horii, Y. Takane, and Y. Isawa, J. Phys. Soc. Jpn. **67**, 1525 (1998).

[43] A. V. Rozhkov, D. P. Arovas, and F. Guinea, Phys. Rev. B **64**, 233301 (2001).

[44] J. A. van Dam, Y. V. Nazarov, E. P. A. M. Bakkers, S. De Franceschi, and L. P. Kouwenhoven, Nature (London) **442**, 667 (2006).

[45] C. Bruder, R. Fazio, and G. Schön, Physica B **203**, 240 (1994).

[46] F. Zhou, P. Charlat, B. Spivak, and B. Pannetier, J. Low Temp. Phys. **110**, 841 (1998).

[47] P. M. Ostrovsky, M. A. Skvortsov, and M. V. Feigel'man, Phys. Rev. Lett. **87**, 027002 (2001).

[48] C. W. J. Beenakker, in *Transport Phenomena in Mesoscopic Systems*, edited by H. Fukuyama and T. Ando (Springer, Berlin, 1992).

[49] O. N. Dorokhov, Solid State Commun. **51**, 381 (1984); P. A. Mello, P. Pereyra, and N. Kumar, Ann. Phys. (N.Y.) **181**, 290 (1988).

[50] We use the same notation for the initial matrix $\hat{A}$ and the rotated matrix $\mathcal{V}^{\dagger}\hat{A}\mathcal{V}$ since they give identical WL corrections and mesoscopic fluctuations.

[51] D. Belitz and T. R. Kirkpatrick, Rev. Mod. Phys. **66**, 261 (1994).

[52] I. L. Aleiner and Ya. M. Blanter, Phys. Rev. B **65**, 115317 (2002).

[53] A. Kamenev, Phys. Rev. Lett. **85**, 4160 (2000).

[54] D. Mailly and M. Sanquer, J. Phys. I **2**, 357 (1992).

[55] B. L. Alt'shuler and B. Z. Spivak, Pis'ma Zh. Eksp. Teor. Fiz. **42**, 363 (1985) [JETP Lett. **42**, 447 (1985)].

[56] S. Feng, P. A. Lee, and A. D. Stone, Phys. Rev. Lett. **56**, 1960 (1986).

[57] B. I. Spivak and S. A. Kivelson, Phys. Rev. B **43**, 3740 (1991).

[58] M. Titov, Ph. Jacquod, and C. W. J. Beenakker, Phys. Rev. B **65**, 012504 (2001).

[59] A. Yu. Zyuzin, B. Spivak, and M. Hruska, Europhys. Lett. **62**, 97 (2003).

[60] M. Abramowitz and I. A. Stegun, *Handbook of Mathematical Functions With Formulas, Graphs, and Mathematical Tables* (Dover, New York, 1964).